

STUDY OF REPULSIVE INTERACTION BETWEEN COLLOIDAL
PARTICLES BY MEANS OF SEDIMENTATION-DIFFUSION-
INTERACTION EQUILIBRIUM UNDER
ULTRACENTRIFUGATION

By

HSIAO-YUAN LI

Bachelor of Science
National Taiwan University
Taipei, Taiwan
1957

Master of Science
Oklahoma State University
Stillwater, Oklahoma
1966

Submitted to the Faculty of the Graduate College
of the Oklahoma State University
in partial fulfillment of the requirements
for the degree of
DOCTOR OF PHILOSOPHY
August, 1969

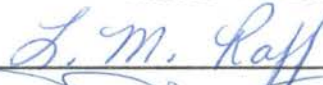
NOV 5 1969

STUDY OF REPULSIVE INTERACTION BETWEEN COLLOIDAL
PARTICLES BY MEANS OF SEDIMENTATION-DIFFUSION-
INTERACTION EQUILIBRIUM UNDER
ULTRACENTRIFUGATION

Thesis Approved:



Thesis Adviser







Dean of the Graduate College

730002

PREFACE

For many years, workers in the field of ultracentrifugation were pre-occupied in the evaluation of molecular weights of macromolecules. Since equilibrium sedimentation methods are time consuming, a very small percent of work was done in this area. It was found that even fewer workers used high concentration samples in their study. In this study, the author realized that the repulsive potential energy between colloidal particles is of the order of that can be attained by spinning a macromolecular sample in an ultracentrifuge. It therefore provides a new method of mapping this energy which for many years does not have a straight forward method of measurement. In order to situate the particles close enough so that interaction can play a part in the equilibrium, sedimentation-diffusion-interaction equilibrium methods always requires very high concentration samples. This is the most essential requirement in the sedimentation-diffusion-interaction technique. In addition to this point, the author wishes also to emphasize here that any small amount of energy comparable to this order of magnitude arising from any other phenomenon should be equally accessible to this technique. There is no reason why its applicability should be limited to electric double layer.

The author wishes first to express his deepest gratitude to Dr. Victor L. Pollak for his guidance and innumerable number of hours of discussion while he was served on my committee. Thanks are next

due to Dr. H. G. Jerrard of the University of Southampton, England, for bring out this problem as well as many valuable discussions when he was a visiting professor at Oklahoma State University. Many thanks are also due to Dr. George Gorin for his kindness to let us use his instrument, without which this work could not possibly be done. Thanks also to my committee members, Dr. H. A. Pohl, Dr. E. E. Kohnke, and Dr. L. M. Raff, for their advices and suggestions. Gratitude shall last, but not least, paid to the Army Research Office at Durham, N. C., the Department of Physics, OSU, for their financial support, as well as the University Computer Center, for the contribution of free computer time.

TABLE OF CONTENTS

Chapter	Page
I. INTRODUCTION	1
Brief Historical Review on Ultracentrifugation	1
Environment Survey, A New Method of Application of Ultracentrifuge	2
II. THEORY	7
Two-Component System vs. Three-Component System	7
The Equation of Motion of Sedimentation-Diffusion- Interaction Equilibrium	11
Derivation of the Interaction Term in the Equation of Motion	14
Verwey-Overbeek's Original Two-Particle Treatment	17
A Suggested Simple Theory	19
III. EXPERIMENTAL	27
Description of Instrument	29
Special Features of Equilibrium Schlieren Curves Involving Interaction	33
Data Reduction	35
Special Consideration on the Sample Concentrations	45
The Salt Effect	46
IV. DISCUSSIONS AND RESULTS	53
Comparison of Experimental and Theory	53
Interaction vs. Buoyancy	56
Prospects of the Sedimentation-Diffusion-Interaction Equilibrium Method	58
A SELECTED BIBLIOGRAPHY	61

LIST OF TABLES

Table	Page
I. Some Properties of Ludox Colloids	28
II. Sample Used for Studying Salt Effect on Interaction Strength	28
III. A Shortened Computer Output Sheet of Numerical Integrations	36
IV. Comparison of Ratios of Experimentally Obtained V_a with Ratios of $1/(1 + \kappa a)^2$	52

LIST OF FIGURES

Figure	Page
1. Comparison of Orders of Magnitude of Electrostatic and Centrifugal Potential Energies on a Small Ion	10
2. Amplitudes of the Solutions of Poisson-Boltzmann Equation of a Confined Spherical Particle	23
3. Electrostatic Potential in a Spherical Double Layer as a Function of Outside Boundary	24
4. A Variable Diopter Prism	29
5. An Equilibrium Schlieren Curve with an Interaction Zone	31
6. Construction Details of (A) the Schlieren System, (B) the Rotor, and (C) the Centrifuge Cell	32
7. The Relationship Between Interacting and Non-interacting Equilibria	40
8. Equilibrium Schlieren Curves of Low Concentration Samples	43
9. The $\log c$ vs. x^2 Plot of a Low Concentration Sample	44
10. Variation of Schlieren Curves as a Function of Small Ion Concentrations in Sedimentation-Diffusion-Interaction Equilibria	48
11. Experimentally Obtained Interaction Potentials	49
12. Equilibrium Schlieren Curve of the Un-treated 15% Ludox SM Sol	50
13. Schlieren Curve of a Sample with a Sufficient Amount of Salt	51
14. Comparison of Theory and Experiment	55
15. Plot of Interaction Potential vs. Buoyancy	59

CHAPTER I

INTRODUCTION

Brief Historical Review on Ultracentrifugation

In 1923, Svedberg and Nichols successfully constructed their first oil-driven 'optical' centrifuge equipment (1) at the University of Wisconsin and coined the word "ultracentrifuge". Immediately afterwards, Svedberg and Fahraeus (2) used this new equipment as a means to determine the molecular weights of macromolecules by sedimentation-diffusion equilibrium. Theories and experimental techniques have been improving constantly since then. However, about two decades ago, there existed less than twenty instruments all around the world. It became a popular research instrument only after the birth of electrically driven ultracentrifuges. At present, several excellent reviews and comprehensive monographs (3, 4, 5, 6, 7) are in existence.

It was found out in the very early stages of development that the system under study must be ideal in order for an accurate determination of molecular weight to be possible. This implies that the macromolecule must not only be charge-neutral, but also satisfy Henry's law (4, 5). As there are seldom any systems satisfying these requirements, considerable effort has been devoted to the

reduction of data (4) in order to obtain a sensibly "good" molecular weight. A very common practice is to run the experiments at several low concentrations and extrapolate the data to zero concentration.

Environment Survey, A New Method of Application of Ultracentrifuge

Extensive references on extracting the molecular weights are available in the literature. In fact, a major part of research in ultracentrifugation in the past was composed of determinations of molecular weights of macromolecules. Besides this application, ultracentrifugation has also been applied occasionally in the studies of decomposition or polymerization of macromolecules (7). No work has been found dealing specifically with the study of environment of the macromolecule.

The author wishes to point out here that centrifugation techniques can be used beneficially in a way totally different from these classical applications¹. Once the molecular weight of a macromolecular species in a system is known to a sufficient degree of accuracy, it can be used as a probe to study the environment of the macromolecule. This concept has been used widely in many fields of physics and chemistry, e.g., in NMR or in Mössbauer effect. However, this capability has not been fully recognized by research

¹Presented at 156th National Meeting, American Chemical Society, Atlantic City, September 8-13, 1968, by Hsiao-Yuan Li and Victor L. Pollak.

workers in ultracentrifugation in the past². Some work on the charge effects in sedimentation velocity has been done by Pederson (8,9,10). However, this is actually a study about the solute-solvent interaction. In general, it can be said that the current common practice in handling non-ideality is to evaluate the second virial coefficient B (13, 14, 15, 16, 17, 18, 19, 20, 21). Besides this, some work has been done by Johnson and coworkers (11, 12) to determine the activity coefficients of systems such as solutions of cadmium iodide or uranyl fluoride. So far the author of this work has found no application using ultracentrifugation to determine the inter-particle potentials, such as the Verwey-Overbeek potential in the double layers.

The centrifugal potential energy difference, with the regular buoyancy term be taken care of, of a macromolecule of average size between the top meniscus and bottom of the cell of a commercially available analytical ultracentrifuge, such as the Beckman Model E, is of the order of a couple of hundreds of kT 's (see Chapter II). If a significant portion of this energy can be conserved and stored as potential energy of interaction between macromolecules by a certain process, this process can be displayed on the schlieren pattern. Taken the simplest case of a two-component system for example, an additional term may be added to take care of the total potential energy of interaction of one macromolecule due to the

²An excellent series of work on sedimentation equilibrium of reacting systems has been published by E. T. Adams, Jr. Thanks are also due to Dr. Adams for calling our attention to the fact that a characteristic schlieren pattern such as shown in Fig.10 & 13 of this work has been observed independently by L. W. Nichol, A. G. Ogston, and B. N. Preston (Biochem. J. 102, 407 (1967)).

presence of other macromolecule (e.g., the Verwey-Overbeek potential). As it will be shown in Chapter II, the equation (2-8) resulting from applying such a correction term in its derivation from a transport approach is identical to the equation obtained from purely thermodynamic approach without using supplementary molecular assumptions. The disadvantages of the transport approach pointed out by Goldberg (22) disappear automatically if one substitutes a soft-ball model with interaction in place of the hard-ball picture.

Earlier works have unfortunately stopped at experimental evaluation of activity coefficients or the virial coefficients, and have made no attempts to relate their data to a basic, specific process. The purpose of the present study is to demonstrate the feasibility of mapping out certain small potentials of interactions not easily accessible by other methods by the method of sedimentation-diffusion-interaction equilibrium, using the Verwey-Overbeek interaction as an example.

Theories on the electric double layer have been worked out extensively by Verwey and Overbeek (23), Deryaguin and Landau (24, 25), and some other workers. Detailed derivations of electric potential, free energy, charge density, etc., based on the Gouy-Chapman model of diffuse double-layer for both flat and spherical geometry of a single particle of low surface potential are given in reference (23). Free energy for two interacting spherical particles only is also given in an approximate form for particles of low surface potentials. The Gouy-Chapman model cannot take the

finite size of ions into consideration, so Stern's correction is usually required for high ion concentrations. Later, in the 1940's, Graham and coworkers improved the theory and found useful applications in electrochemistry (26, 33). Graham's theory fits the electro-capillary data much better than the original ones. However, due to the complexities involved, no attempt to use Graham's theory will be made. In the present work, the author wishes only to demonstrate that sedimentation equilibrium can be used fruitfully in this area and leave the detailed refinement to future works.

It is well known that theories related to the properties of electric double-layer still need a more straightforward, direct, critical experimental check³. Sedimentation equilibrium opens a path for it. Also for this reason, the subject of experimental verification of V. O. theory was picked up in this study. It is clear that the use of sedimentation-diffusion-interaction equilibrium method is not limited to this area only, although good agreement between theory and experiment was observed in

³As reflected in the recent symposiums on colloidal electrolytes at the 154th, 155th, and 156th ACS National Meetings, light scattering, surface tension, and electrophoretic mobility data are still among the important experimental criteria used to check the validity of theories on electric double-layer. None of these provided accurate enough comparison between theory and experimental at present. At the 156th ACS National Meeting, considerable attention was given to the derivation of isotherms from the theories. However, difficulties preventing straightforward comparison between theories and experiments still existed as a major problem. One may need as many more assumptions to get the isotherm equation from double-layer theory as one needs to derive the theory of double-layer itself.

this area.

In Chapter II, the equation for sedimentation experiments involving inter-particle interaction (the sedimentation-diffusion-interaction equilibrium equation) will be derived first. A simple approach for deriving the interaction potential from electrostatics will also be suggested.

In Chapter III, experimental procedures and results will be given. Special considerations on the unusual experimental conditions will be emphasized. Method of data reduction will also be given in this chapter.

Chapter IV contains the comparison of theory and experiment as well as a discussion of discrepancies. Some discussion on the relation of this experiment to the buoyancy phenomena will also be given in this chapter. A brief conclusion and expectations on future developments of the sedimentation-diffusion-interaction equilibrium method will be presented in Chapter IV also.

CHAPTER II

THEORY

In this chapter, comparison of the orders of magnitude of the electrostatic energy and gravitational energy of small ions and macromolecules will first be made. Such a comparison will allow us to justify the use of the assumption that, in the analysis of experiments involving colloids such as the "Ludox SM" sols which were used here, the system under study can be treated as a two-component system (solvent and particle) with the addition of an extra interaction potential between particle and particle, or between particle and solvent, rather than be treated conventionally as multi-component system (i.e., the particles, the solvent, and the small ions). Next, based on balancing the material transported across an area perpendicular to the radius vector, an equation of motion which includes the overall inter-particle interaction potential shall be derived. In addition to this, a simple theory to calculate this potential from electrostatics will then be derived. Comparison of theory and experiment will be discussed in Chapter IV.

Two-Component System vs. Three-Component System

Let us assume there are i kinds of particles in the solution. In general, this includes the colloid particles (the macromolecular ions), the positive, and the negative small ions. We shall not

consider the solvent molecules except in the discussion of buoyancy. That is to say, the particle-solvent interaction will be generally neglected in this case.

Under thermodynamic equilibrium, all these particles are expected to follow Boltzmann distribution

$$N_i/N_{oi} \approx \exp(-\Delta E_i/kT) \cdot g_i/g_{oi}, \quad (2-1)$$

where N_{oi} is the number of particles of the i th kind at the reference point of E_i , and the g 's are the degeneracy factors. ΔE_i is commonly split into several terms, each of which may arise from a different source. The energy sources which contribute significantly to the systems under the existing experimental conditions are the gravitational (centrifugal) and electrostatic energies. Thermal energies (translational, rotational, and vibrational) also contribute a large portion of the total energy. However, since their averages are not functions of space coordinates, its contribution to the ΔE_i term will not give the sort of distribution of our interest. (Thermal equilibrium between the macromolecular ions and the small ions is reached predominantly through collisions with solvent molecules rather than mutual collisions.)

For a macromolecule of molecular weight $M = 220,000$ amu, of density $\rho = 2.20$ gm./c.c., and spinning at a speed of 12,000 rpm, the gravitational energy difference between the top meniscus and bottom meniscus of the sample section of the ultracentrifuge cell is approximately $100 kT(3.7 \times 10^{-12} \text{ erg.})^1$. While for small ions, this

$$^1 (M/N_A) \cdot (1 - \rho_o/\rho) \omega^2 (x_b^2 - x_o^2) = (220,000/6.023 \times 10^{23}) \times$$

term is 10^{-4} times smaller (0.01 kT). On the other hand, a preliminary calculation (27) showed the electric potential energy for a mono-valent ion due to diffuse double layer has a maxima of approximately 7 kT's near the surface of a Ludox SM particle (see Fig. 1). A comparison of the magnitudes of gravitational energy and electric energy for the small ions will lead us to two conclusions of considerable significance to experimental work. The very large mass to charge ratio of macromolecules plays a useful role here on the difference of behavior under centrifugal force.

In the absence of charged macromolecules or particles, the concentration difference of small ions between two meniscuses (due to redistribution under centrifugation) is less than 1% of the original concentration before centrifugation. (Special cases such as those in the density gradient technique, in which heavy small ions such as Cs^+ were used may be exceptions.) Since the original concentration of small ions in any stable sol is rather small (approximately 0.001 mole), it is not expected that the redistribution of small ions would be observed through the schlieren optical system.² Furthermore, since the ion concentration did not change very much, its effect on the behavior of the colloid can be neglected.

Next, the electrostatic energy change across the dimension

$$(1 - 1/2.20) \times (2\pi \times 12,000/60)^2 \times (7.03^2 - 6.2^2) / (1.38 \times 10^{-16} \times 293) \\ = 102.6 \text{ kT.}$$

²It may be observable by using the Rayleigh interferometer. However, the Rayleigh interferometer is not suitable for measuring the high concentrations of the colloidal sols.

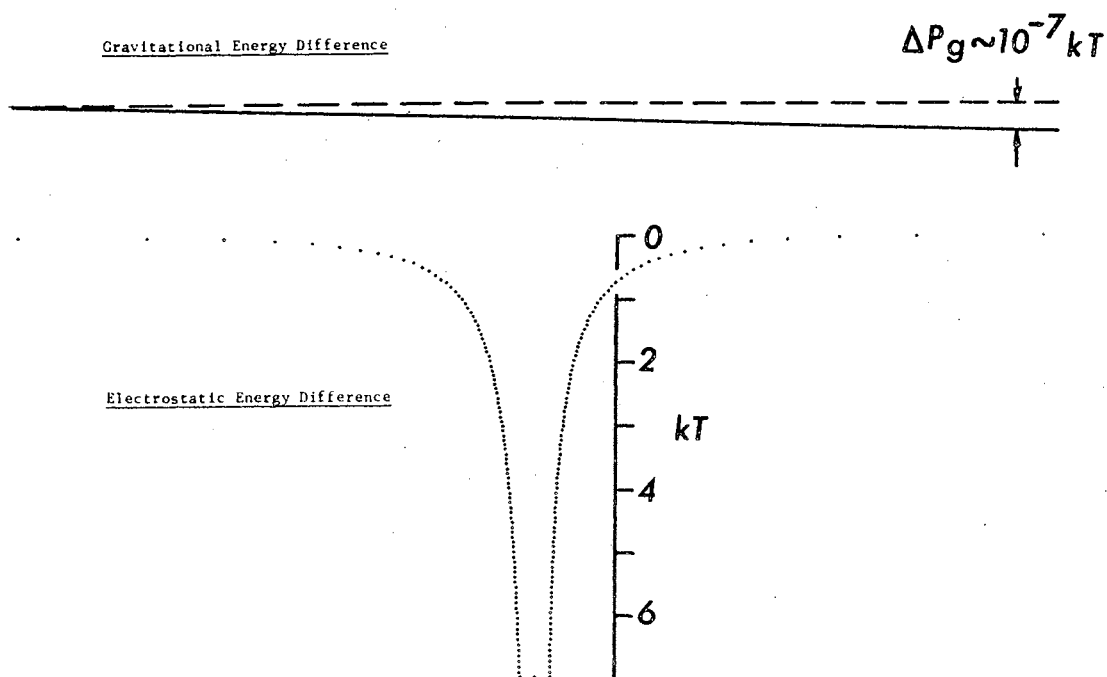


Figure 1. Comparison of Orders of Magnitude of Electrostatic and Gravitational Potential Energies on a Small Ion Located in the Bulk Liquid³.

occupied by one macromolecule and its surrounding small ions is of the order of 7 kT's, while the gravitational energy change across the same dimension is approximately equal to 0.01 kT times the

³In Figure 1, the diameter of the particle is approximately equal to the nearest gap between the two branches of the dotted curve. The farthestmost points plotted are 15 times the particle diameter away from the center. The electrostatic energy was calculated on an IBM-1620 according to the method given in Reference 36 and subsequently plotted on a Calcomp 565 digital plotter. The surface charge density was chosen from a typical case, such as that given on P. 58 of Ref. 36. The small ion concentration at the bulk was calculated from du Pont data sheet. The gravitational energy was plotted on an exaggerated scale. The solid curve for the gravitational energy is actually a segment of a parabola which passes through the energy scale zero at the center of rotation.

ratio of the diameter of this volume to the cell length (this ratio is of the order of 10^{-6}). We can therefore conclude that the gravitational energy term can be neglected in setting up the Poisson-Boltzmann equation, and the movements of small ions are governed only by the electrostatic potential to a high degree of approximation. In other words, the "symmetry" character of the distribution of small ions has not been destroyed by the superposing of a centrifugal force. The charged cloud formed by small ions can thus be considered as moving along with the macromolecule during the course of sedimentation. That is, the macromolecule and the small ions can be treated as a single body in the analysis of their motion. This conclusion is in agreement with the results of measurements of emf generated in the centrifuge cell during sedimentation (28, 29). Matsukura reported a value of approximately 24 mv for bovine serum albumin at pH 2.0 and 9780 rpm. Such a small voltage certainly can not be expected to produce large electrophoretic actions. This further convinces us that the colloid system can be handled as a two-component system. The effect of the small ion cloud is included in the interparticle potential. This approach will reduce considerably the complexity of mathematical analysis.

The Equation of Motion of Sedimentation-Diffusion-Interaction Equilibrium

If Coriolis and radial accelerations are neglected, the forces experienced by a macromolecule after the rotor reaches the desired speed are the centrifugal force \vec{G} , buoyancy force \vec{B} ,

frictional force \vec{F} , and a force due to interactions \vec{I} . The equation of motion is obtained directly from the condition

$$\vec{G} + \vec{B} + \vec{F} + \vec{I} = 0. \quad (2-2)$$

The interaction term can further be split into two terms

$$\vec{I} = \vec{I}_s + \vec{I}_m.$$

where \vec{I}_s comes from the macromolecule-solvent interaction, and \vec{I}_m comes from the mutual interaction between macromolecules. Here it has been assumed for simplicity that only one kind of macromolecule is present in the sample. The macromolecule-solvent interaction term plays an important role only in sedimentation velocity experiments. Fixman (46) was able to show that, in the particular case of a single-solvent system, all macromolecule-solvent interactions in sedimentation-equilibrium experiments may be made to vanish identically by taking the density of the solvent as the density of the medium in the buoyancy term.

It has been a common practice to reduce the \vec{I}_m term as much as possible by using dilute macromolecule solutions. When the required dilution cannot be achieved experimentally without hurting the accuracy of ultracentrifugation data, the residue effects due to the presence of \vec{I}_m are normally taken care of either by taking the density of solution (i.e., the average density of macromolecules and bulk liquid) as the density of the medium, or by defining an apparent diffusion constant for the macromolecule, or by applying both. The validity of such practices are not always clear from doubt. In the past, both the density of the solvent and the density of the solution has been widely used in the literature as the density of the medium (5,52,54,55).

In our opinion, whether the density of the solution can be used as the density of the medium depends on the fact whether the macromolecule sees the surroundings as a uniform medium or not. In a colloidal sol with low ion concentrations, the electrical double-layer thickness is usually very large and the force between macromolecules is of long-range character. Therefore, the particle is not likely to see a uniform environment. Experiment shows that this is the case (Fig. 15). The inclusion of I_m into the buoyancy term will lead to a complicated pseudo-buoyancy phenomenon. We shall therefore separate these two terms and write

$$\begin{aligned} \vec{G} &= m\omega^2 \vec{x} \\ \vec{B} &= -m\rho_0 \bar{V}\omega^2 \vec{x} \\ \vec{F} &= -f\vec{x} \end{aligned} \tag{2-3}$$

and

$$\vec{I}_m = - \frac{\partial V_T}{\partial \vec{x}}$$

where m is the molecular weight of the macromolecule; ω is the angular velocity in rad./sec; x is the distance between the particle and the center of the rotor; ρ_0 is the density of the solvent; \bar{V} is the specific volume of the macromolecular solute; f , the friction coefficient; and V_T the total potential energy of one macromolecule due to the presence of other macromolecules.

Equation (2-2) can then be written as

$$m(1-\bar{V}\rho_0)\omega^2 \vec{x} - f\vec{x} - \frac{\partial V_T}{\partial \vec{x}} = 0 \tag{2-4}$$

The last term in (2-4), or more generally, the underlined terms in Equations (2-4), (2-7) and (2-8), are new terms which did not appear in the conventional treatment. As usual, we shall couple Equation

(2-4) with the overall mass-current density (Equation 2-5) flowing across a surface located at x and perpendicular to the radius vector,

$$\vec{J} = c\vec{x} - D\nabla c, \quad (2-5); \quad fD = kT, \quad (2-6)$$

and the Einstein relation (2-6)

$$m(1 - \bar{U}\rho_o) \omega^2 x = \frac{\partial V_T}{\partial x} + \frac{kT}{c} \frac{\partial c}{\partial x} \quad (2-7)$$

$$\frac{1}{2}m(1 - \bar{U}\rho_o) \omega^2 (x^2 - x_1^2) = \frac{V_T[c] - V_T[c_o(x_1)]}{c} + kT \ln \frac{c(x)}{c_o(x_1)} \quad (2-9)$$

Equation (2-7) results from eliminating x and fd from (2-4), (2-5), and (2-6), and is easily integrable to Equation (2-8). This equation is identical to the Equation (7) given by Goldberg (22), except that he expresses the right-hand terms in terms of activity coefficient.

Conventionally, an equation of motion (3, 6) is obtained by setting the Lamm equation equal to zero and combining it with the Svedberg equation:

$$\frac{1}{2}m(1 - \bar{U}\rho_o) \omega^2 (x^2 - x_1^2) = kT \ln \frac{c(x)}{c_o(x_1)} \quad (2-10)$$

such an equation does not contain the V_T terms. This is due to the difference between the soft-ball picture and the hard-ball picture. When the hard sphere approximation is made, the excess chemical potential term of the solutes automatically vanishes (22) from the equation. Equation (2-8) reduces to Equation (2-9) at very low concentrations since the V_T terms become smaller and smaller as the interparticle distance increases.

Derivation of the Interaction Term in the Equation of Motion

It is now necessary to derive V_T in Equation (2-8) from fundamental electrostatic considerations. Before we start the derivation,

we shall briefly review the works published in the literature.

Progress in the ideas related to the electrical double-layer has been quite slow. Gouy⁽³⁰⁾ and Chapman⁽³¹⁾ proposed independently the first model as early as 1913 (the diffuse double-layer theory). Stern modified the Gouy-Chapman model in 1924⁽³²⁾ by considering the finite size of ions (the compact double-layer theory). A monograph was published in 1948 by Verwey and Overbeek⁽²³⁾, summing up the details of the theory to date. This is usually cited as the Verwey-Overbeek theory or the Derjaguin-Landau-Verwey-Overbeek theory⁽²⁴⁾⁽²⁵⁾. Quite apart from this line of development, S. Levine and his school held a rather different point of view^(37,38,39,40,41,42). They fought their way from the very beginning up to very recent days⁽⁵¹⁾. In short, it can only be said that the great debate has not yet been settled. On the other hand, Graham and coworkers perfected the theory and the experimental technique of capillary electrometer^(26,33) of dropping mercury electrode. Bibliographs in the application of electric double-layer theory to the electrode kinetics can be found in Delahay's book⁽³³⁾. Further theoretical work after the publication of Verwey-Overbeek's book can be traced back from the recent Russian monograph⁽³⁴⁾. However, direct experimental verification of these theories is still in the primitive stages⁽³⁵⁾.

As is well known, the classical analysis of the diffuse double-layer leads to the Poisson-Boltzmann equation (2-10). In mks units, this equation looks like the following:

$$\nabla^2 \psi = \frac{2evn}{\epsilon} \sinh \frac{ev\psi}{kT}, \quad (2-10)$$

where e is the elementary charge, and v is the valance of the ions (assumed to be the same for both positive and negative ions in this equation). The Poisson-Boltzmann equation does not possess analytical solutions for particles of spherical geometry. Analytical solutions have so far been obtained for certain special cases such as:

- (1) the flat double layer, and
- (2) the spherical double layer with small surface potential.

In the second case, the Poisson-Boltzmann equation was linearized by taking only the first term in the expansion of the hyperbolic sine function. Such a procedure is often called the Debye-Huckel approximation. Although this approximation is far from satisfactory, it provides a simple and useful method of comparing numerical data. If solutions for the un-linearized equation is required, the aid of a digital computer is always sought (36) 4.

Verwey and Overbeek computed in their book the free energy of interaction of two (and only two) spherical particles by some approximate methods. However, they did not consider the case of many particles situated around a central particle, which is actually more realistic. In the next section, a very brief summary of the results of Verwey-Overbeek's two particle treatment will be given, and then, in the section following, a very simple model to solve the same problem will be proposed. The simplicity of this model led us to believe that this is a very good order-of-magnitude calculation

⁴The results given in Ref. (36) were reproduced by the author on the IBM-7040 at the OSU Computer Center. However, the corrections are rather small in most cases and it was found more convenient not to use it.

and very useful for making comparison with the experimental data at the early stages of development of this technique.

Verwey-Overbeek's Original Two-Particle Treatment

Verwey and Overbeek calculated the potential energy of interaction of two spherical double layers in their book. The derivation is quite lengthy; therefore, no attempt is made to duplicate it here. Readers who are interested in it should read the original literature (see Chapter X, §§2,3, Reference 23). They have given the repulsive potential of interaction in two cases of two identical double layers having a small electrical potential Ψ near the solid-liquid interface, that is, for the double layers where the linearized Poisson-Boltzmann equation can be used. These are: (A) where the surface electric potential is assumed constant, or (B) where the surface charge is assumed constant at the approaching of the particles. The results are given below:

(A) The Case of Constant Electric Potential at the Surface

$$\begin{aligned} V_{R(\Psi_0=\text{const})} &= \Psi_0(Q_{\infty} - Q_R) \\ &= \Psi_0^2 \epsilon a \frac{e^{-\tau(s-2)}}{s} \beta \end{aligned} \quad (2-11)$$

in which

$$\beta = \frac{1 + \alpha}{1 + \frac{e^{-\tau(s-2)}}{2s\tau} (1 - e^{-2\tau})(1 + \alpha)} \quad (2-12)$$

(B) The Case of Constant Surface Charge.

$$\begin{aligned}
 V_{R(Q=\text{const})} &= Q(\Psi_R - \Psi_\infty) \\
 &= \Psi_0^2 \epsilon a \frac{e^{-\tau(s-2)}}{s} \gamma
 \end{aligned}
 \tag{2-13}$$

in which

$$\gamma = \frac{1 + \alpha}{1 - \frac{e^{-\tau(s-2)}}{2s\tau} \left(\frac{\tau-1}{\tau+1} + e^{-2\tau} \right) (1 + \alpha)}
 \tag{2-14}$$

In both cases, where $\alpha = \lambda_1 \left(1 + \frac{1}{s\tau}\right) + \lambda_2 \left(1 + \frac{3}{s\tau} + \frac{3}{(s\tau)^2}\right)$

(2-15)

in which λ_1 and λ_2 are the roots of a set of simultaneous equations obtained from a lengthy calculation (see Equations 71 and 72 in Reference 23).

The symbols used in the above equations have the following meanings:

a	is the radius of the particle
$s=R/a$	the interparticle distance (center to center) measured in terms of radius of the particle
$\tau=\kappa a$	the radius of the particle measured in Debye length
Ψ_0, Q	surface potential and surface charge, respectively
ϵ	dielectric constant
β and γ	factors of order 1 defined in Equations (2-13) and (2-13) respectively

A Suggested Simple Theory

In the following, we shall suggest a simple theory regarding a colloidal particle occupying only a limited space. Since in any actual case, a colloidal particle has its neighbors surrounding it, a case such as that described in the last section does not exist. In the last section, only two particles are assumed embedded in an infinitely large bulk of liquid. In an actual case, since the concentration is never zero, each particle can only occupy a limited volume of space. As a colloid particle, along with its surrounding small ions, sediments towards the "bottom" of the centrifuge cell, the volume occupied by each particle diminishes. The requirement of charge neutrality means that the charge cloud of the diffuse layer must be squeezed into a smaller volume. We shall discuss the change of free energy during such a process.

Now let us introduce a macromolecular particle of total surface charge Q at the origin of a coordinate system. Around the particle, in an infinitely large amount of solution of positive and negative ions, each of a concentration of n ions/c.c., is a handful of counterions whose total charge is $-Q$. These charges will be assumed to distribute themselves according to the answers obtained by Loeb, Overbeek, and Wiersema⁽³⁶⁾. The electrostatic potential at infinity is set equal to zero for convenience.

Next, let the charge cloud be redistributed such that it occupies only a volume of finite radius b . We can then reduce b to achieve the effect of squeezing. As long as b is sufficiently

large, the potential and charge distribution are good approximations to the case of infinite radius.

Let us further assume that the effects of volume reduction and particle crowding can be approximated by a symmetrical reduction of radius b , which calls for a spherically symmetrical modification of the electrostatic potential Ψ . We shall expect here that a model based on spherical symmetry will give certain discrepancies.

In addition to the above assumptions, let us further assume that the Debye-Huckel approximation is applicable. We shall first obtain the expression for ϕ .

Instead of using the Dirichlet boundary conditions as they are often employed in literature on theories of electric double layer, let us apply the Neumann boundary conditions

$$\left(\frac{\partial\phi'}{\partial r}\right)_b = 0, \quad \left(\frac{\partial\phi'}{\partial r}\right)_a = -\frac{4\pi\sigma}{\epsilon} \quad (2-16)$$

to the linearized Poisson-Boltzmann equation

$$\nabla^2\phi = \kappa^2\phi, \quad \text{where} \quad \kappa^2 = \frac{2eV_0n}{\epsilon kT} \quad (2-17)$$

The first boundary condition comes from the symmetry relationship between any two particles and the second, from Gauss' law. We shall, for the moment, assume that σ is constant during the squeezing process although it may not correspond to the true physical situation due to the involvement of chemical reactions on or near the surface. The solution of this boundary value problem should also be subject to all the limitations of applicability inherent in the Gouy-Chapman model.

Change the variable φ' in (2-17) to $u = r\varphi'$, the equation reduces to

$$\frac{d^2}{dr^2} u = \kappa^2 u$$

The general solution of this equation is

$$u = Ae^{-\kappa r} + Be^{\kappa r} \quad (2-18)$$

Since we are interested only in the region between $r = a$ and $r = b$, the second term $Be^{\kappa r}$ will not give an un-physical result. So

$$\varphi' = \frac{Ae^{-\kappa r}}{r} + \frac{Be^{\kappa r}}{r} \quad (2-19)$$

The boundary conditions (2-16) require that

$$\begin{aligned} A(1 + \kappa b)e^{-\kappa b} + B(1 - \kappa b)e^{\kappa b} &= 0 \\ A(1 + \kappa a)e^{-\kappa a} + B(1 - \kappa a)e^{\kappa a} &= \frac{4\pi\sigma a^2}{\epsilon} = \frac{Q}{\epsilon} \end{aligned}$$

which gives

$$A = \frac{\frac{Q}{\epsilon} (1 - \kappa b)e^{\kappa b}}{(1 - \kappa b)(1 + \kappa a)e^{\kappa(b-a)} - (1 + \kappa b)(1 - \kappa a)e^{\kappa(a-b)}} \quad (2-20)$$

$$B = \frac{-\frac{Q}{\epsilon} (1 + \kappa b)e^{-\kappa b}}{(1 - \kappa b)(1 + \kappa a)e^{\kappa(b-a)} - (1 + \kappa b)(1 - \kappa a)e^{\kappa(a-b)}} \quad (2-21)$$

As $b \rightarrow \infty$, $A \rightarrow \frac{Q}{\epsilon} \frac{e^{\kappa a}}{1 + \kappa a}$ and $B \rightarrow 0$ which is identical with the

answers given by Verwey and Overbeek.⁵

The values of $\frac{A\epsilon(1+\kappa a)}{Qe^{\kappa a}}$ and $\frac{B\epsilon(1+\kappa a)}{Qe^{\kappa a}}$ are plotted in

Fig. 2 as a function of κb for $\kappa a = 0.1$. It is interesting to notice the contribution due to the first term of Equation (2-19) decreases as κb decreases, and passes through a value 0 at $\kappa b = 1.0$. It is in fact opposite in sign from that of second term for $\kappa b < 1.0$.

Some values of Ψ 's are plotted in Fig. 3 for $\kappa b = 1.0, 1.2, 1.5, 2.0$ and ∞ . Fig. 3 indicates that, if Q is kept constant, the absolute value of the surface potential increases as κb decreases. Or more precisely, the ratio of surface potential to surface charge increases as the "free" volume available to each particle decreases. In Verwey-Overbeek's original calculations, in which they always used the Dirichlet boundary conditions, either the surface potential or the surface charge is assumed constant. The author feels that such assumptions do not correspond to the experimental conditions of this study, although such assumptions may be true for some electrode kinetics experiments.

Verwey and Overbeek suggested two expressions for the Helmholtz free energy for the diffused double layer⁽³⁷⁾, which shall be written down without proof in the following:

⁵Equation (15) of Reference 23 gives

$$\Psi = \Psi_a \frac{a}{r} e^{-\kappa(a-r)}$$

where Ψ_a and Q are related by the equation

$$Q = \epsilon a (1 + \kappa a) \Psi_a$$

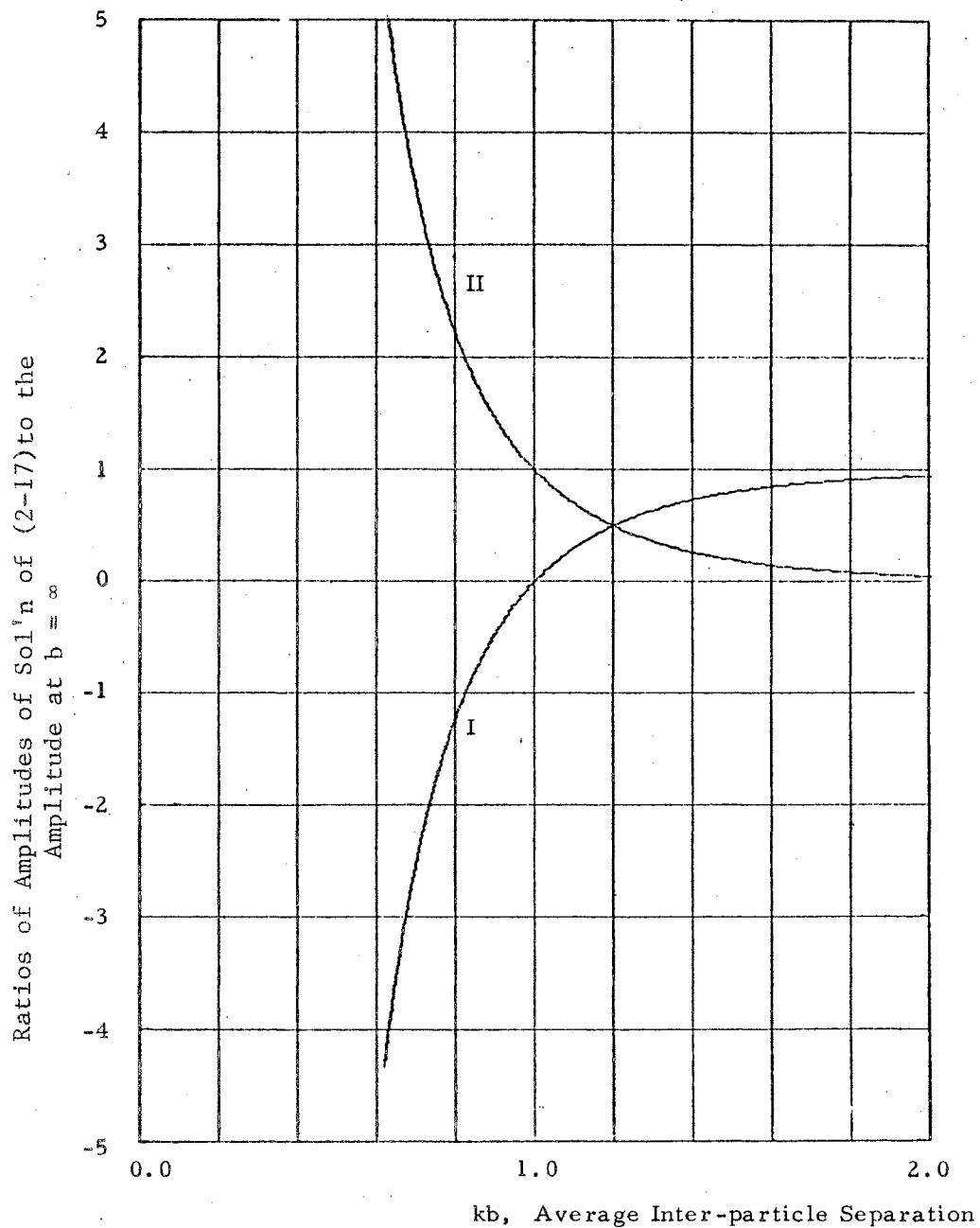


Figure 2. Amplitudes of the Solutions of Poisson-Boltzmann Equation of a Spherical Particle of Radius $\kappa a = 0.1$ (in Debye length) Confined in a Volume of $(4\pi/3)b^3$.
 (I), $A\epsilon(1+\kappa a)/Qe^{\kappa a}$; (II), $B\epsilon(1+\kappa a)/Qe^{\kappa a}$.

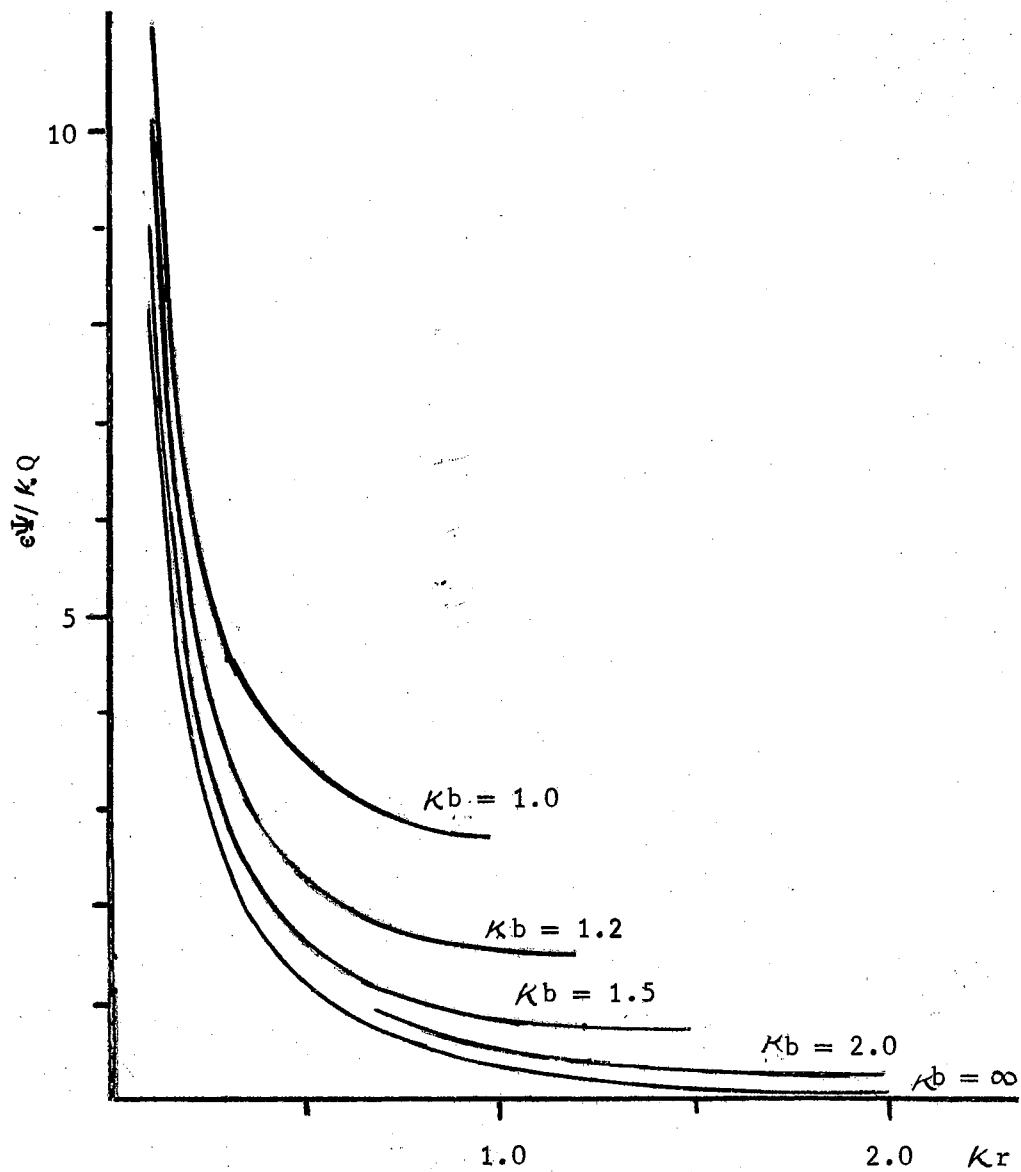


Figure 3. Variation of Electrostatic Potential in a Spherical Double Layer as a Function of Outside Boundary Expressed in Debye Length.

$$F = - \int_S dS \int_0^{\Psi_0} \sigma' d\Psi' \quad (2-22)$$

$$F = \int_0^1 \frac{d\lambda}{\lambda} \iiint \Psi' (x, y, z) \rho' (x, y, z) dx dy dz \quad (2-23)$$

where Ψ_0 is the surface electric potential, σdS is the charge of a surface element dS , ρ' and Ψ' are the charge density and electric potential corresponding to an ionic charge λe , which increases from zero to the full value of e .

Since they give this expression in a rather intuitive way, it has drawn certain criticism in the past ^(38, 39, 40, 41, 42). Ikeda tried to put Equation (2-22) and (2-23) on the basis of strict statistical mechanics ⁽⁴³⁾. He succeeded in deriving Equation (2-22), but failed to obtain an identical result for Equation (2-23). A series of papers on the statistical theory of double layer has been published by Martynov ⁽³⁴⁾. At the present, this is an area still not satisfactorily settled. For the purpose of this research, we shall be content to use the simple expression (2-22), since the free energy evaluated from this equation agrees with experimental data (Fig.15).

From very fundamental consideration of electrostatics ⁽⁴⁴⁾, the free energy contributed by a distribution of charges can be written in the two integrals as the charge and potential gradually build themselves up to their full value.

$$\frac{1}{2} \int \sigma \Psi_a ds \quad (2-24)$$

$$\text{and} \quad \frac{1}{2} \int \rho \Psi dV \quad (2-25)$$

using the Ψ obtained from last section in the above equations, the surface integral shows an increase in free energy as the "free" volume is reduced, while the volume integral causes a decrease in the free energy of the system. However, Ikeda has in fact shown that the volume integration is a part of the expression of entropy derived from statistical mechanics. Except for a surface integral term on the outside boundary of the "free" volume (this term has only small contributions), Ikeda's derivation is applicable to the Von Naumann's boundary conditions (2-16) with only small errors introduced by the finite size of outer boundary. We have therefore evaluated the free energy from (2-19), (2-20), (2-21) and (2-24). The values are plotted along with experimental data in Fig. 15.

It is important to notice here that the calculated free energy is only a weakly varying function of Q/κ . By proper adjustment of these two parameters, a very close fit can be achieved in a wide range of concentrations of macromolecules. The calculated values deviate from experimental data, more seriously at the higher end, in the region of small inter-particle distance. This is just as was expected since in this region the Debye-Huckel approximation fails to describe the situation.

CHAPTER III

EXPERIMENTAL

Silica sols of nominal seven millimicron diameter (du Pont Ludox SM¹) were used in this study. Ludox is well known for its use as a light-scattering standard for molecular weight determination(49). A study by Alexander and Iler (50) also revealed that the particles are of rather uniform diameters under electron microscope. The general properties of these sols can be found in the du Pont product bulletins(57). The part of the data in which we are interested in this work is listed in Table I. Du Pont manufactured two forms of Ludox SM; the more recent one has a silica content of 30% by weight, while the older one contains only 15% solid. Both forms were used in this study. The 30% sample was diluted to one half of its original strength for ease of comparison. The variation of interaction as a function of small ion concentrations was investigated by adding various amounts of sodium chloride (see Table II) to the 30% Ludox SM sol during dilution.

¹These sols are made by growing amorphous silica around hard spherical nuclei which were obtained by passing sodium silicate solution through an ion-exchanger (47,48). The designations used in type classification of Ludox are: HS - high sodium stabilization level; LS - low sodium stabilization level; SM - seven millimicron diameter; AM - alumina modified; and AS - ammonia stabilized.

TABLE I

SOME PROPERTIES OF LUDOX COLLOIDS (at 25°C)

Type of Colloid ¹	HS	LS	SM	AM	AS
Approx. Part. Diam. (m μ)	14-15	14-15	7-9	14-15	14-15
pH	9.9	8.3	8.5	9.1	9.6
Total Na ⁺ Ions/cc (10 ¹⁷)*	120	15	4.5	17.7	7.5
Surface Charge Density* (Coul./m ²)	-0.155	-0.050	-0.055	-0.066	-0.232
Debye Length κ^{-1} (in m μ)*	2.16	6.14	25.6	5.65	8.4
Surface Potential * (in $y_0 = eV_0/kT$)	5.86	5.68	7.07	6.06	9.44

*See Reference No. 27.

TABLE II

SAMPLE USED FOR STUDYING SALT EFFECT ON INTERACTION STRENGTH

Sample No.	I	II	III	IV
Solid Content (% wt)	16.37	15.64	14.65	14.10
NaCl Added (N)	.0071	.0143	.0285	.0446
$\kappa = \frac{1}{\text{Debye Length}}$ (x10 ⁶ /cm)	2.90	4.10	5.79	9.05

Description of Instrument

A standard analytical ultracentrifuge (Beckman Model E) was used throughout the study. Because of the unusual requirement of high sample concentrations, it is expected that if best results are to be obtained, certain modifications of the existing instrument needs to be carried out². Unfortunately, this is not easily accomplished. The author has thus limited himself to the use of the existing instrument and its parts available on the market. This

²For best results, the overall aperture of the optical path of the instrument should be enlarged. An alternative but easier way to modify the instrument is to install a variable diopter prism in the optical path with its controller mounted in the front panel. A variable diopter prism is a device composed of two wedge-shaped prisms capable of rotating opposite to each other simultaneously in a plane perpendicular to the optical axis. The prisms should be mounted above the vacuum chamber in a position as far below the phase analyzer as possible. Such an assembly will sacrifice certain conveniences but it will permit us to take pictures of different portions of schlieren curve on separate photographic frames of those normally hidden in the concentration band. A trial run was carried out by hanging a fixed diopter wedged prism of 3.0 to 4.0 diopter in the slit holder inside the vacuum chamber. It did help estimate the height of the maximum point of the schlieren curve which normally swings out of view during the trial period of the experiment in establishing the optimistic conditions of operation. However, such a setup is difficult to handle and hazardous; therefore, it has not been used to collect data.

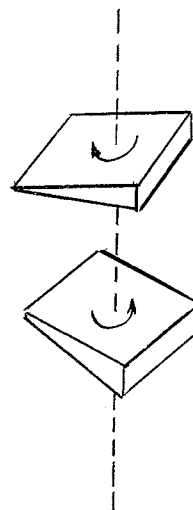


Figure 4. A Variable Diopter Prism.

undoubtedly will narrow the range of investigation.

The Beckman Model E, manufactured by the Spinco division, has 60 adjustable steps of pre-selected speed ranging from as low as 1967 rpm up to 72,140 rpm. The An-D analytic rotor attachment has a recommended maximum operating speed of 59,780 rpm. Each centerpiece or cell window has its own recommended maximum speed. Three optical systems are provided with the instrument to measure the concentration gradient and/or the concentration at any point in the cell during the run at a distance r from the center of rotation -- the schlieren optics, the Rayleigh interferometer, and the UV absorption system. For the sample used in this study and for the range of concentration gradient which is required to measure, the schlieren optics is the most suitable. The author shall not describe the principles of the system since these are easily available elsewhere⁽⁴⁵⁾³.

The schlieren curves are recorded on Kodak, extra-high contrast, metallographic plates. The curve height as a function of radial positions are read afterwards from a Starrett micrometer with the aid of a projector. The micrometer has an precision of 0.0002 of a millimeter. It is believed that, in the majority of the curve, an accuracy of one-thousandth of a millimeter is always achieved. An equilibrium schlieren curve is shown in Figure 5, and the

³Experimental procedures can also be found in great detail in Reference (45). A diagram of the schlieren system used in the instrument is reproduced in Figure 6.

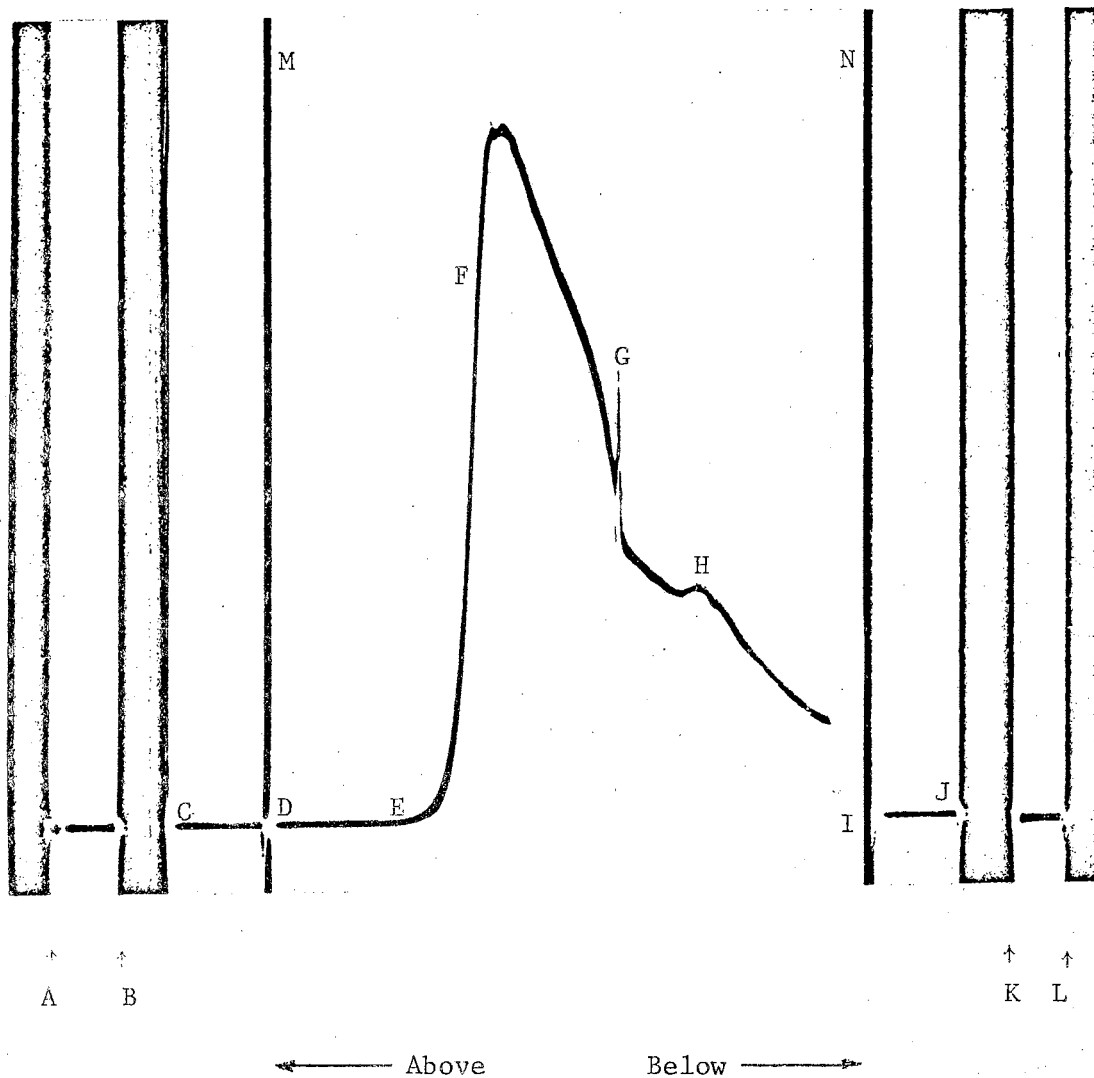


Figure 5. An Equilibrium Schlieren Curve with an Interaction Zone.

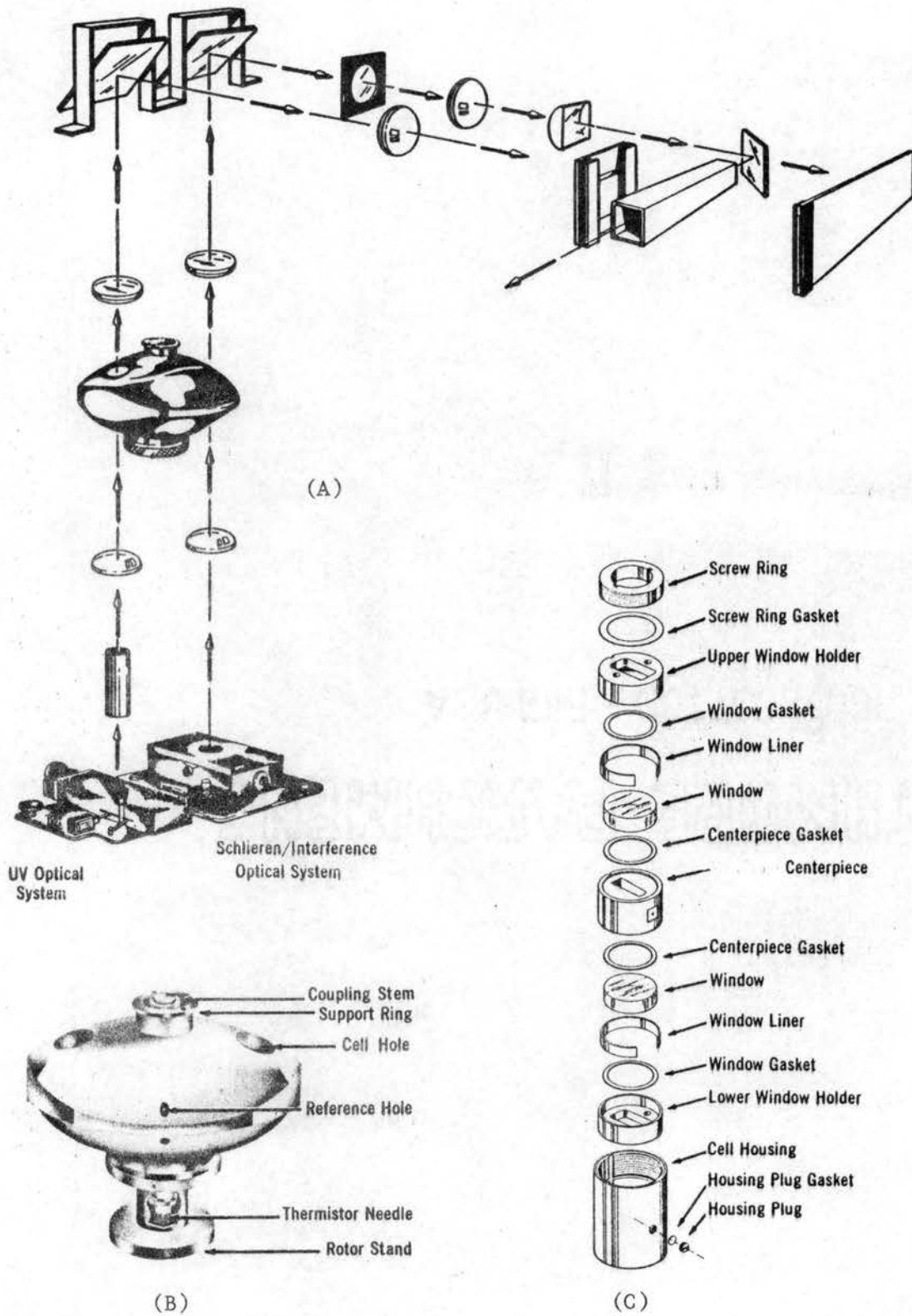


Figure 6. Construction Details of (A), the Schlieren System, (B), the Rotor, and (C), the Centrifuge Cell.

construction of the rotor and the cell, as well as the schlieren system, are shown in Figure 6. The cell centerpiece has a sectorial cross-section. A filled Epon centerpiece of 3 mm thickness and 4° sector angle was used for high concentration samples, while a 12 mm, 2° sector angled filled Epon centerpiece was used for low concentration samples. All experiments were carried out at 20°C under the thermister temperature controlling system of the "Model E".

Special Features of Equilibrium Schlieren Curves Involving Interaction

Figure 5 shows certain features which do not normally show up during an ordinary run. However, these special features made this picture particularly useful for illustration purposes. The sample used in this picture is a Ludox SM of original 30% by weight silica content and diluted to one-half of this strength. This sample was allowed to spin long enough so that coagulation started at the bottom part of the cell. The spaces between points A and B, and points K and L are the reference holes of the reference cell, which is in a vacuum of approximately 1 millitorr. The center of rotation is located at 5.70 cm to the left of point B. MD and NI are the shadows of the top and the bottom meniscuses respectively. For most runs of this study, the cell space between the bottom meniscus I and the cell bottom J are filled with a heavy transparent compound⁴ FC-43 to create a clear bottom. It is worth

⁴FC-43 is a 3M product which has a density of 1.872 and refractive index of 1.2910 at 25°C . This oil is formed from tributylamine with fluorine replacing the hydrogen atoms.

noticing here that the density of FC-43 is lower than the density of solid silica, yet the surface tension still keeps the silica particles floating on top of a lighter liquid.

The space CD above the sample is an air space sealed into the cell at one atm. The schlieren curve DEFGHI can be broken into five portions. The portion DE is essentially horizontal and the concentration of macromolecule in this region is very close to zero. EF is the sedimentation-diffusion equilibrium region. The width of this region measured along the radius vector has been observed increasing as the speed of rotation decreases. In fact, if one gradually reduces the speed as well as the sample concentration in a sequence of runs, region EF becomes wider and wider, and it eventually covers the whole depth of the sample region (from D to I), and becomes identical to any normal equilibrium schlieren curves frequently reported in the literature. This phenomenon can easily be understood if one recalls that the horizontal axis (radial distance) can also be considered as the energy axis, and that the schlieren curve plotted on an uniform energy axis is a unique curve independent of speed rotation.

Region FG is the sedimentation-diffusion-interaction equilibrium region. This is the region where interaction shows its effect. The slope of the schlieren curve, i.e., the second partial derivative of concentration with respect to radial distance, may vary in a very wide range as the strength of interaction varies.

A comparison of Figures 10, 12, and 13 against Figure 5 will make this point clear. The monotonic increasing feature found in sedimentation-diffusion equilibrium schlieren curves was destroyed by the interaction. This is a very important feature of equilibrium schlieren curves involving interactions, and is a very useful experimental criterion to identify the region.

Regions GH and HI normally do not appear; however, this picture was taken after running over a week purposely to allow coagulation to be recorded on the photograph. After stopping the rotor, we found that the region HI was actually filled with a solid, glass-like stuff, while a very viscous heavy fluid was found in the region GH. The relative relationship can almost be maintained undisturbed if one stops the rotor without using heavy braking. This can be indicated by the fact that the schlieren curve quickly reaches a steady state within 30 minutes after re-starting the rotor. The new schlieren curve thus obtained is almost identical to the equilibrium curve before the rotor was brought to a stop. We suggest tentatively that in zone GH the sample is polymerizing (coagulating), while in zone HI it is polymerized (coagulated). The exact nature of these zones is not fully understood.

Data Reduction

A typical read-out of the schlieren curve from the micrometer consists of a few hundreds of pairs of x-y coordinates. (See Table III for an example of a shortened computer output of numerical integration.) The abscissae are measured from the outer edge of

TABLE III. A SHORTENED COMPUTER OUTPUT SHEET
FOR NUMERICAL INTEGRATION.

DATE AND SAMPLE NUMBER 660913.3
 PICTURE FRAME NUMBER 11
 ANGULAR VELOCITY 12590. RPM
 TIME AFTER REACHING SPEED 736. MINUTES
 LOCATION OF TOP MENISCUS 5.9315 CM. FROM CENTER OF ROTATION
 LOCATION OF BOTTOM MENISCUS 7.0394 CM. FROM CENTER OF ROTATION
 POINT WHERE INTEGRATION STARTED 6.1743 CM. FROM CENTER OF ROTATION

RAD. DIST.	SCHLIEREN	CV HT.	RAD DIST SQ.	1ST INTEG.	2ND INTEG.
0.6174300E 01	-0.		0.3812198E 02		
0.6198015E 01	-0.		0.3841539E 02	-0.	
0.6221714E 01	0.6000005E-02		0.3870972E 02	0.7109703E-04	0.5225122E-05
0.6245389E 01	0.2100001E-01		0.3900488E 02	0.3907094E-03	0.3925144E-04
0.6269013E 01	0.5500000E-01		0.3930053E 02	0.1288432E-02	0.1632804E-03
0.6292536E 01	0.1270000E 00		0.3959601E 02	0.3429017E-02	0.5122496E-03
0.6315984E 01	0.2270000E 00		0.3989166E 02	0.7579350E-02	0.1326021E-02
0.6339448E 01	0.3210000E 00		0.4018860E 02	0.1400854E-01	0.2922502E-02
0.6362990E 01	0.3860000E 00		0.4048764E 02	0.2233049E-01	0.5621364E-02
0.6386593E 01	0.4280000E 00		0.4078857E 02	0.3193689E-01	0.9679661E-02
0.6410212E 01	0.4640000E 00		0.4109081E 02	0.4247095E-01	0.1527896E-01
0.6433836E 01	0.4980000E 00		0.4139425E 02	0.5383423E-01	0.2255753E-01
0.6457458E 01	0.5330000E 00		0.4169876E 02	0.6601118E-01	0.3165043E-01
0.6481082E 01	0.5670000E 00		0.4200442E 02	0.7900453E-01	0.4269204E-01
0.6504695E 01	0.6050000E 00		0.4231106E 02	0.9284211E-01	0.5582577E-01
0.6528296E 01	0.6480000E 00		0.4261864E 02	0.1076277E 00	0.7119588E-01
0.6551891E 01	0.6930000E 00		0.4292727E 02	0.1234481E 00	0.8896674E-01
0.6575488E 01	0.7370000E 00		0.4323704E 02	0.1403204E 00	0.1093205E 00
0.6599075E 01	0.7850000E 00		0.4354779E 02	0.1582700E 00	0.1324470E 00
0.6622659E 01	0.8340000E 00		0.4385962E 02	0.1773615E 00	0.1585238E 00
0.6646246E 01	0.8820000E 00		0.4417259E 02	0.1975991E 00	0.1877571E 00
0.6669833E 01	0.9300000E 00		0.4448667E 02	0.2189689E 00	0.2203537E 00
0.6693415E 01	0.9800000E 00		0.4480180E 02	0.2414893E 00	0.2565126E 00
0.6716994E 01	0.1031000E 01		0.4511800E 02	0.2651979E 00	0.2964335E 00
0.6740578E 01	0.1080000E 01		0.4543539E 02	0.2900911E 00	0.3403329E 00
0.6764162E 01	0.1129000E 01		0.4575389E 02	0.3161399E 00	0.3884389E 00
0.6787749E 01	0.1177000E 01		0.4607354E 02	0.3433357E 00	0.4409533E 00
0.6811339E 01	0.1224000E 01		0.4639433E 02	0.3716550E 00	0.4980936E 00
0.6834928E 01	0.1271000E 01		0.4671624E 02	0.4010830E 00	0.5600706E 00
0.6858515E 01	0.1319000E 01		0.4703923E 02	0.4316281E 00	0.6270892E 00
0.6882102E 01	0.1367000E 01		0.4736333E 02	0.4633054E 00	0.6993564E 00
0.6905694E 01	0.1413000E 01		0.4768861E 02	0.4960986E 00	0.7770964E 00
0.6929316E 01	0.1448000E 01		0.4801542E 02	0.5298894E 00	0.8605357E 00
0.6952908E 01	0.1494000E 01		0.4834293E 02	0.5645936E 00	0.9499612E 00
0.6976468E 01	0.1552000E 01		0.4867111E 02	0.6004759E 00	0.1045360E 01
0.7030423E 01	0.1706980E 01		0.4942685E 02	0.6883947E 00	0.1151117E 01
TOTAL AREA OF 2ND INTEGRATION 0.1151117E 01					
PROP. CONST. (C/C(0)/1ST INTEG.) 0.6242318E 01					

the inner reference hole, i.e., from point B in Figure 5. This point is physically located at a distance of 5.700 cm from the center of rotation. If only one cell contains sample, the other position on the rotor usually contains a reference cell which has two built-in reference holes and a center hole which holds a counter-weight. In the case that two samples are running simultaneously, the reference cell is replaced by a cell with wedge-shaped window, and an outer reference hole drilled into the rotor is un-plugged to provide the standard point of distance measurement. Due to the enlarging factor of the optical system, the x-distance measured on the photographic plate should be multiplied by a factor of 0.4743 to convert it to the actual physical distance along the radius of the rotor.

The ordinates listed in Table III are proportional to the partial derivatives of the refractive index with respect to radial distance of the sample at the points of interest, which in turn are proportional to the concentration gradient. The proportionality constant should contain such factors as the thickness of the centerpiece, the initial concentration of the sample, the specific refractive index, the y-enlarging factor of the optical system (which is different from the x-enlarging factor because a cylindrical lense is used in the schlieren system), and a tangent function of the schlieren angle setting. Fortunately, one does not have to deduce this constant from all these factors. It may simply be obtained by comparing the total mass of macromolecules in the

sample to the second integration of schlieren curve height expressed in arbitrary unit with respect to radial distance. The concentration of the sample at each point along the radial distance can then be obtained by multiplying the proportionality constant just obtained to the first numerical integration of the experimental data. If a geometrical "lattice" pattern is assumed on the relative locations of the particles, the average interparticle distance can then be estimated from concentration information. If we agree that there is no permanent structure between colloidal particles, a definite geometrical pattern would be impossible to assign. However, since the distances calculated from unit cells of constant volume using different space point groups differ from each other only by a factor of unity, we may simply use a cubic lattice and leave a correction factor open.

To evaluate the interparticle interaction potential from experimental data, one can follow the reasoning below: From Eq.(2-8), it is seen that

$$\begin{aligned} \Delta V &= V_T [c(x)] - V_T [c_o(x_1)] \\ &= \frac{1}{2}m(1 - \bar{v}\rho_o)\omega^2(x^2 - x_1^2) - kT \ln \frac{c(x)}{c_o(x_1)}, \end{aligned} \quad (3-1)$$

where x_1 is a reference point on the radius vector where the concentration of the sol at equilibrium equals the initial concentration before spinning. All the rest of notations are identical to those used in Chapter II. It is worth noticing at this point that the right hand side of Eq. (3-1) contains only the experimental data.

For an ideal case such as those described by Eq. (2-9), in which inter-particle interactions are not present, the left-hand side of Eq. (3-1) should be zero and the concentration of the macromolecules at sedimentation-diffusion equilibrium is governed by the equation

$$c(x) = c_0(x_1) \exp \left[\frac{-m(1 - \bar{v}\rho_0)\omega^2(x^2 - x_1^2)}{2kT} \right], \quad (3-2)$$

which, if plotted on a semi-log scale of c vs. x^2 , gives a straight line. Let us recall that this is one of the standard procedures for determining the molecular weight of macromolecules. The slope of the semi-log plot is a measure of the molecular weight.

Since we are normally operating at a speed much higher than those in the conventional practice, a zero concentration region is developed near the top meniscus (the region DE in Fig. 5), the region immediately below is bound to have very low concentration and can therefore be used for molecular weight evaluation for checking purpose, and for providing a reference line for interparticle potential evaluation. This point has been confirmed since the particle diameter evaluated from this region agrees very well with the nominal size of the particle (Table I). It agree also very well with the special runs on low concentration samples carried out to check the molecular weight of the sample and the degree of poly-disperse (Fig. 9).

As one goes further toward the bottom of the cell, the concentration of the macromolecule becomes higher and the inter-

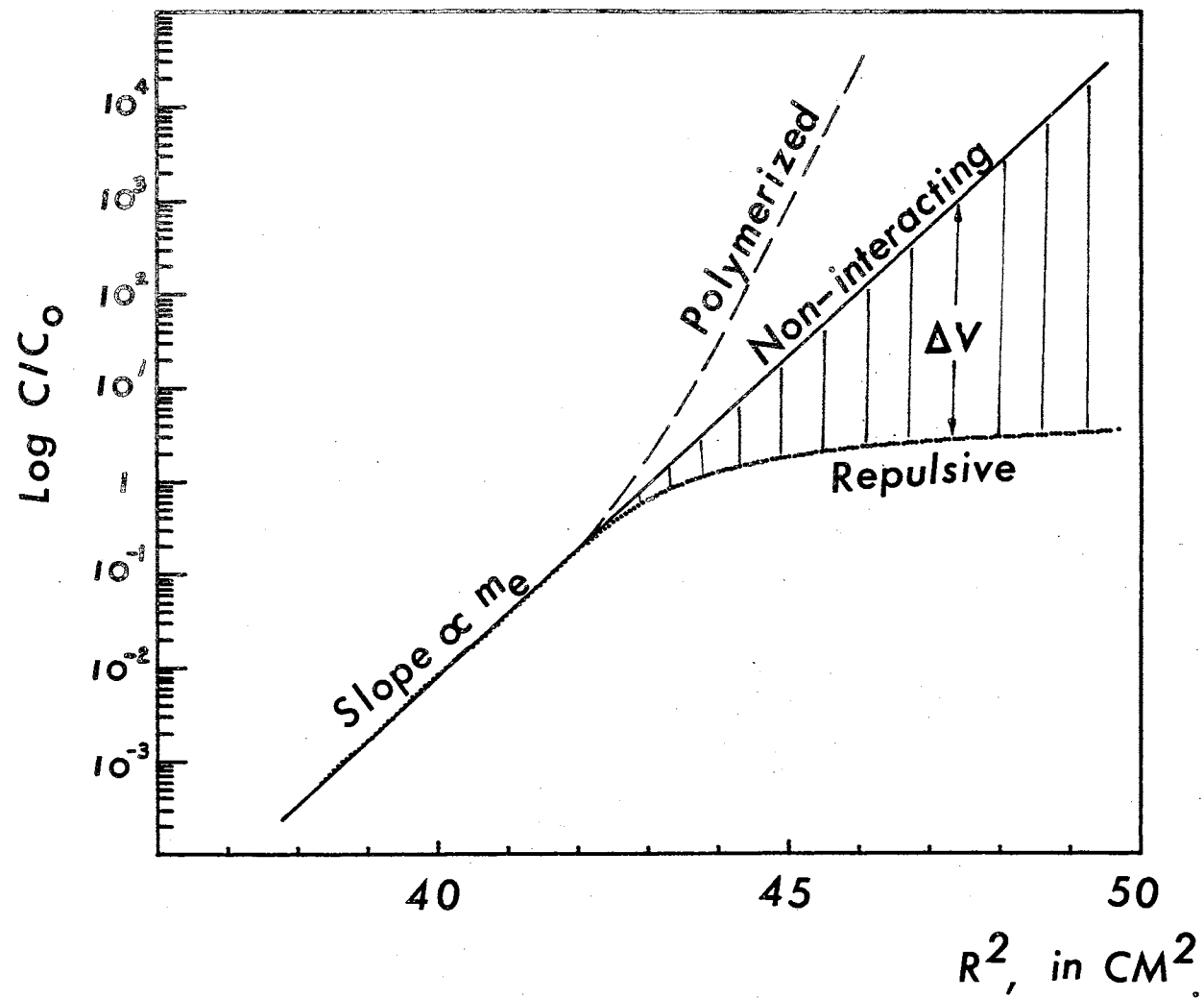


Figure 7. The Relationship between Interacting and Non-interacting Equilibria.

particle interaction starts playing a part. We can thus predict that a deviation from the straight-line plot of $\log c$ vs x^2 should occur in this high concentration region. This is found to be the case. (See Fig. 10; also the dotted points in Fig. 7.) A comparison of Eq. (3-2) with Eq. (2-8) shows that the deviation from the straight line is the term ΔV in Eq. (3-1). Thus the straight line obtained from the lower-concentration portion of the schlieren curve should be extrapolated and the differences between this line and the experimental data line should be assigned to ΔV .

Now there is enough information to plot the total inter-particle interaction as a function of average inter-particle distance. Let us remember here that the ΔV thus obtained is purely experimental. It is therefore very clear that the procedure to obtain it is independent of any theory regardless the nature or source of the interaction.

The ideas discussed above can be summarized in Fig. 7. In this plot, the dots are experimental points derived from a typical ultracentrifuge run whose schlieren curve is shown in Fig. 12. In the left portion of the curve, i.e., in the lower concentration region, the points lie on a very good straight line. If such a non-interacting situation were to continue into the higher concentration region, the experimental curve would coincide with the extended straight line in the right portion of the curve. However, the observed curve shows that it bends downward to the right, which indicates that the sample possesses a repulsive inter-particle

potential⁵.

In order to further assure that the downward bending of Fig. 7 at the high concentration region is not due to sample inhomogeneity, two samples of 1.28% and 3.80% by weight respectively were run at 2,378 rpm. These are the conventional conditions of operation for sedimentation-diffusion equilibria. If the bending were due to the redistribution of inhomogeneous particles, the same characteristics would be observed for both the low and high concentration samples. The schlieren curves of the low concentration runs are shown in Fig. 8. These resemble any normal schlieren curves for sedimentation-diffusion equilibria published in the literature. The $\log c$ vs x^2 curve for one of the low concentration samples is shown in Fig. 9. Since the concentration of macromolecules at the top meniscus can no longer be assumed zero at such a low speed of rotation, top meniscus concentration corrections are required for all experimental points.

A set of programs was written to handle the numerical integrations and other data reduction calculations. The programs were run on the IBM-7040 computer of the University Computer Center at Oklahoma State University. When plotting was required, a card deck was normally produced by the 7040 and brought to the Engineering Computer Laboratory where plots were made on a Calcomp 565 digital incremental plotter driven on-line by an IBM-1620 computer.

⁵Ikeda and Kakiuchi reported some polymerized samples whose curves of $\log c$ vs x^2 bend upward. See Reference 56.

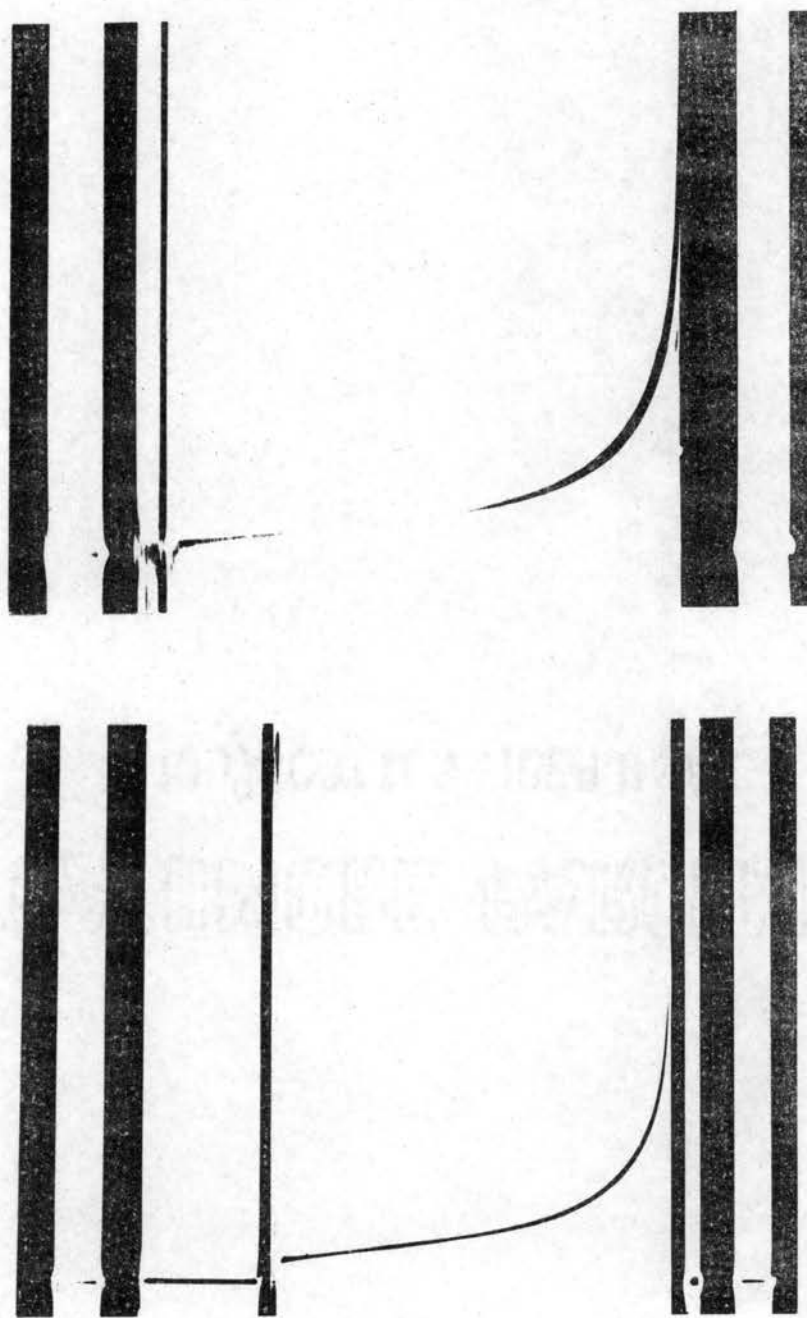


Figure 8. Equilibrium Schlieren Curves of Low Concentration Samples.

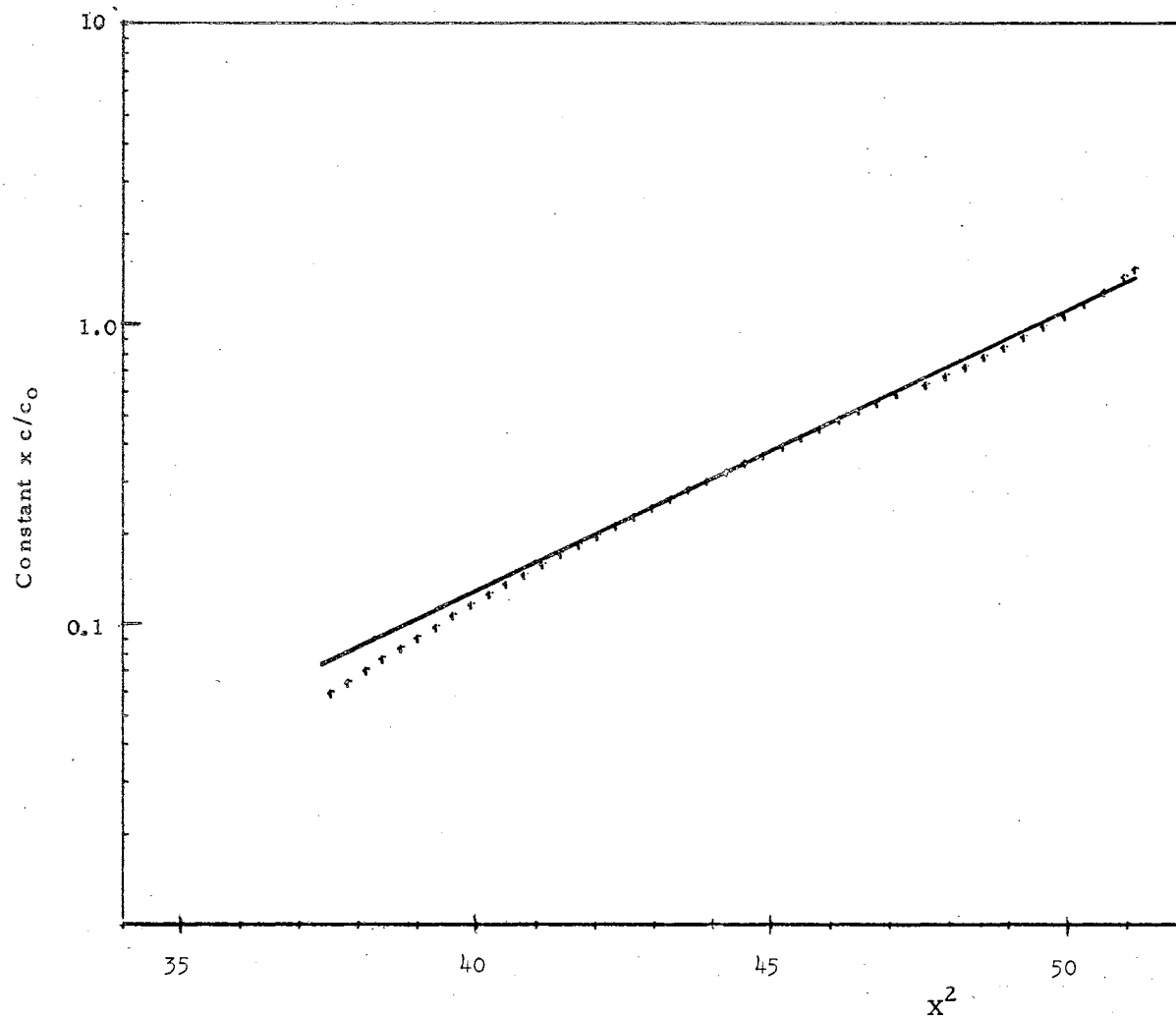


Figure 9. The $\log c/c_0$ vs x^2 Plot of the Diluted Ludox SM Sol, whose Schlieren Curve is Shown in the Lower Part of Fig. 8. A concentration of $0.033xc_0$ is assumed at the top meniscus. The slope of the straight line corresponds to a molecular mass of 3.7×10^{-19} gm.

Special Considerations on the Sample Concentrations

Because of the fact that interaction becomes a major factor only at a rather short inter-particle distance, it becomes measurable only after the particles approach each other close enough so that the effect of diffusion does not overshadow the effect of interaction. Therefore, it is required to carry out the experimental studies of inter-particle interaction by ultracentrifuge methods at high macromolecular concentration. The author wishes to emphasize here that such a requirement in the experimental conditions is a rather un-conventional approach since traditionally there is a habit to carry out ultracentrifugation tests at low concentrations⁶.

Furthermore, the "equilibrium method" is clearly favored over the velocity method since one does not have to consider the dynamic aspects in the process of sedimentation. The author wishes also to emphasize here that equilibria of this type are not reached by balances of the sedimentation and diffusion processes; these are rather sedimentation-diffusion-interaction equilibria. Experimentally, it means that the centrifugation must be carried out at a speed much greater than that suitable for conventional sedimentation-diffusion equilibrium studies⁷. This high speed is essential to push the

⁶Most analytical ultracentrifuge samples have a concentration range of 0.5% by weight of macromolecule or less.

⁷For example, the Beckman Instrument Corp. recommended the speed for sedimentation equilibrium runs be calculated from the formula: $\text{rpm} = 8.165 \times 10^5 / \sqrt{M(1 - \rho_p)}$. For a sample of $M = 220,000$ (that of Ludox SM), the calculated speed should be 2,357 rpm. However, a successful run requires the speed be set between 6,000 to 13,000 rpm.

mutually repulsive particles together. A more favorable experimental condition is to set the instrument at an even higher speed so that the whole diffusion region is moved away from the top meniscus. Such a practice has the advantage of an easier numerical integration since we can then set both the concentration and the mass of macromolecule at the top meniscus to zero.

The ideas which we discussed here can be made more clear if the reader refers back to Fig. 7 and the last two sections of this chapter.

One of the obvious disadvantages of using high-concentration samples is that the schlieren pattern may easily be thrown out of the view because of the limited aperture size of the optical system. This results a dark (unlighted) concentration band on the photograph. By properly reducing both the spinning speed and the thickness of the centerpiece of ultracentrifuge cell⁸, it is possible to bring the whole range of the schlieren curve into the view for the smaller particle-size samples made from Ludox SM. However, it has been found difficult to bring the whole view of the schlieren curves into the scope properly for samples made of larger particles such as the Ludox HS or the light scattering standard Ludox.

The Salt Effect

A series of sedimentation-diffusion-interaction equilibrium

⁸Three mm is the minimum thickness for the filled Epon centerpieces available from Spinco. Although an 1.5 mm aluminum centerpiece is also available, it does not satisfy the purpose because of corrosion.

experiments were carried out on the 30% by weight Ludox SM samples diluted to 15% with salt water. (See Table II for salt content). The schlieren curves are shown in Fig. 10. This type of the schlieren curves with a maximum near the bottom of the cell has been reported only very recently by Nichol, Ogston, and Preston (53), who were also able to bring out the part of the schlieren curve normally hidden in the concentration band. The finding of this study confirmed that their observation is really a wider class of new phenomenon which might draw sufficient interest in the field of ultracentrifugation.

The interparticle potentials obtained experimentally by the method described in a previous section of this chapter are plotted in Fig. 11. In Table IV, the Debye lengths κ^{-1} calculated from the added salt concentrations were presented. The Verwey-Overbeek potential at the surface of the particle obtainable from Eq. 2-13 should be proportional to the factor $1/(1 + \kappa a)^2$. Therefore, we extrapolated the potential in Fig. 11 to 7 m μ inter-particle distance. The ratios are presented in the last line of Table IV. It can be seen that agreement with the ratios of $1/(1 + \kappa a)^2$ is quite good. The discrepancy is believed to be due to the inaccuracy of the extrapolation and the inaccuracy of the initial salt concentrations in the samples.

The 15% Ludox SM sol (original concentration) behaved quite differently before salt was added. (See Fig. 12 for its schlieren curve.) However, when enough salt was added to the sample, a schlieren

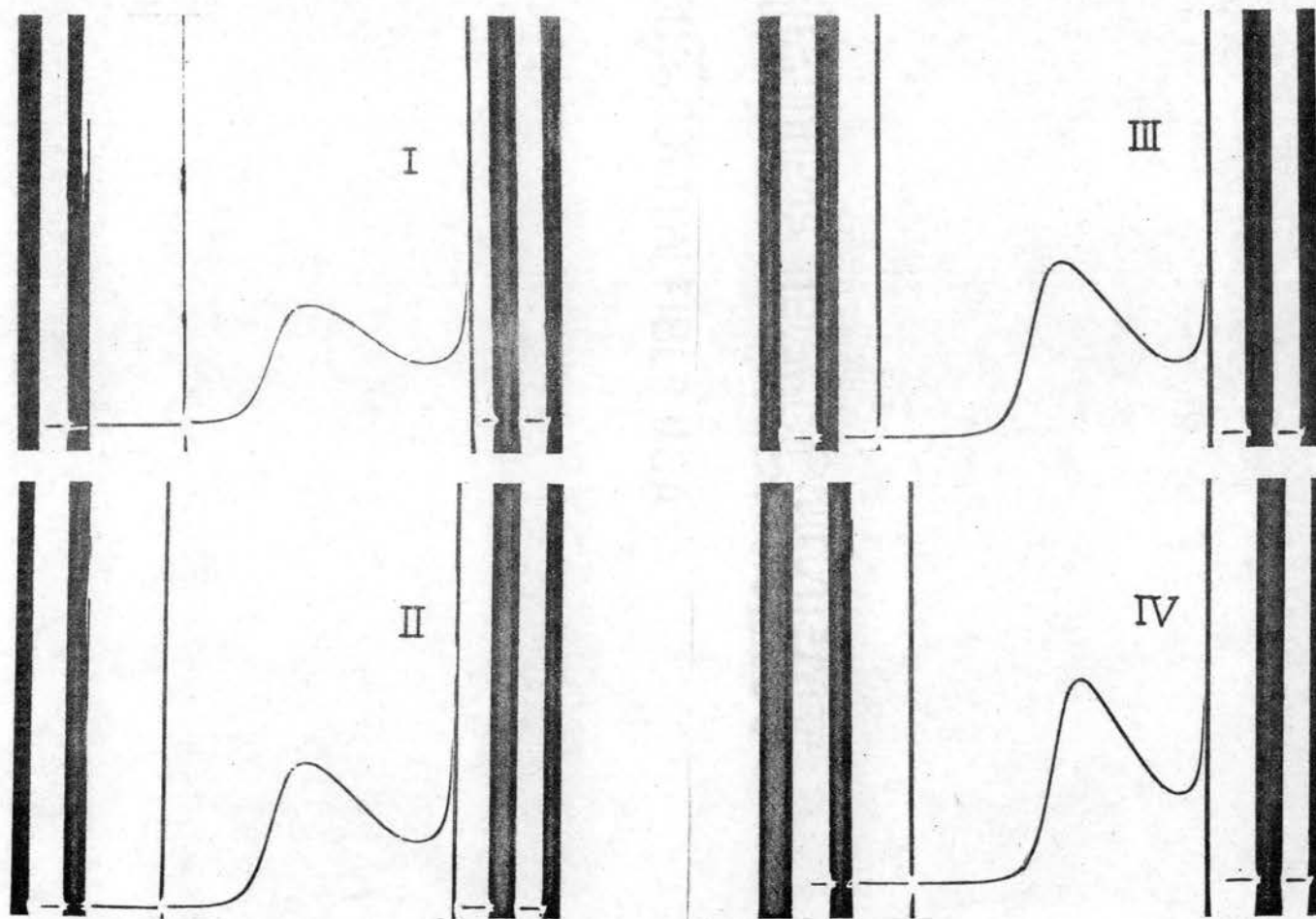


Figure 10. Variations of Sedimentation-Diffusion-Interaction Equilibrium Schlieren Curves as a Function of Small Ion Concentrations.

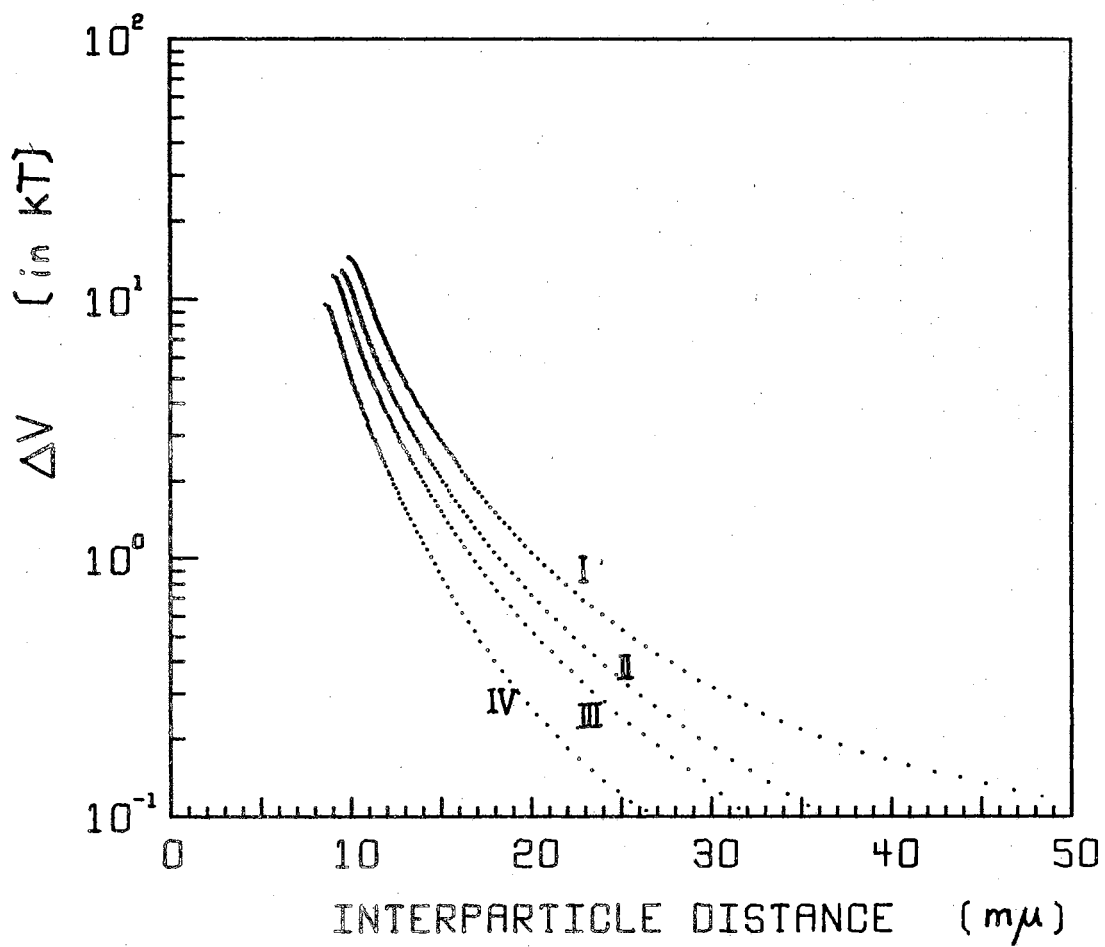


Figure 11. Experimentally Obtained Interaction Potentials for the Samples whose Schlieren Curves are Shown in Fig. 10.

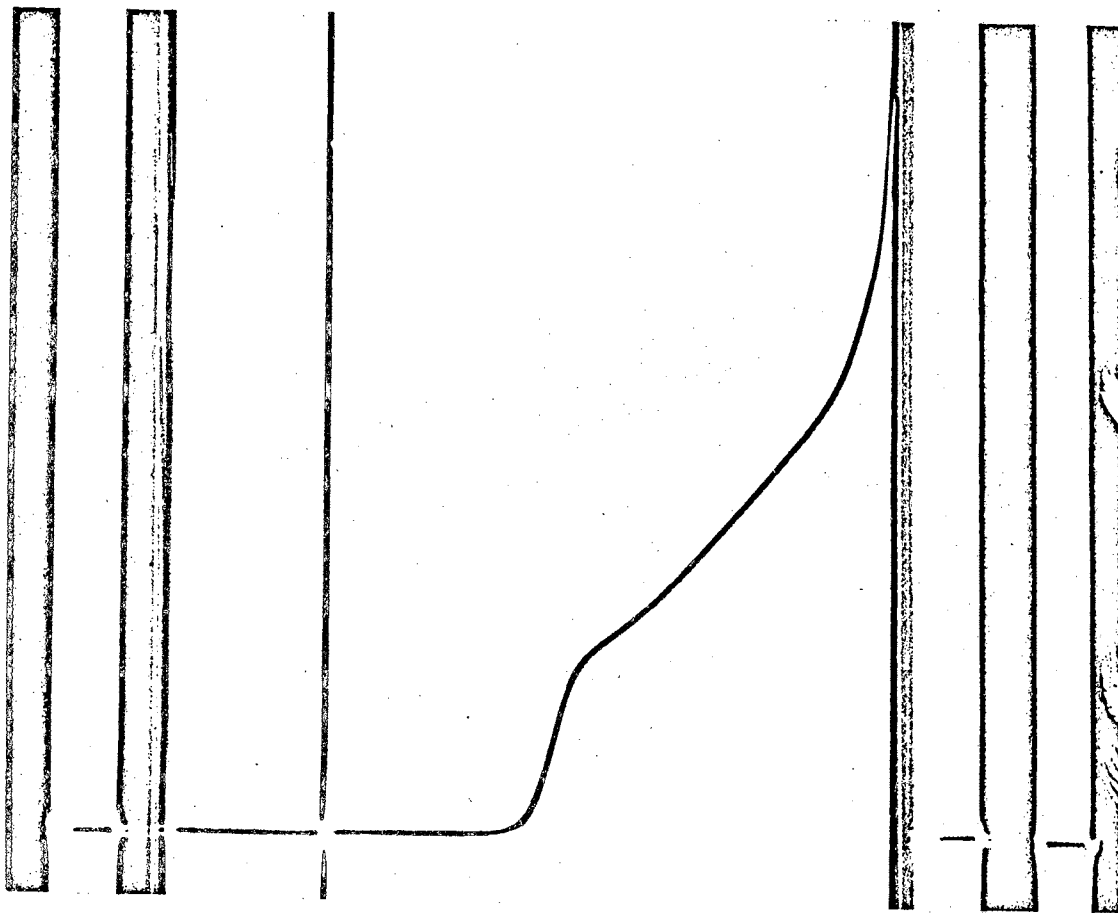


Figure 12. Schlieren Curve of the Un-treated 15% Ludox SM Sol.

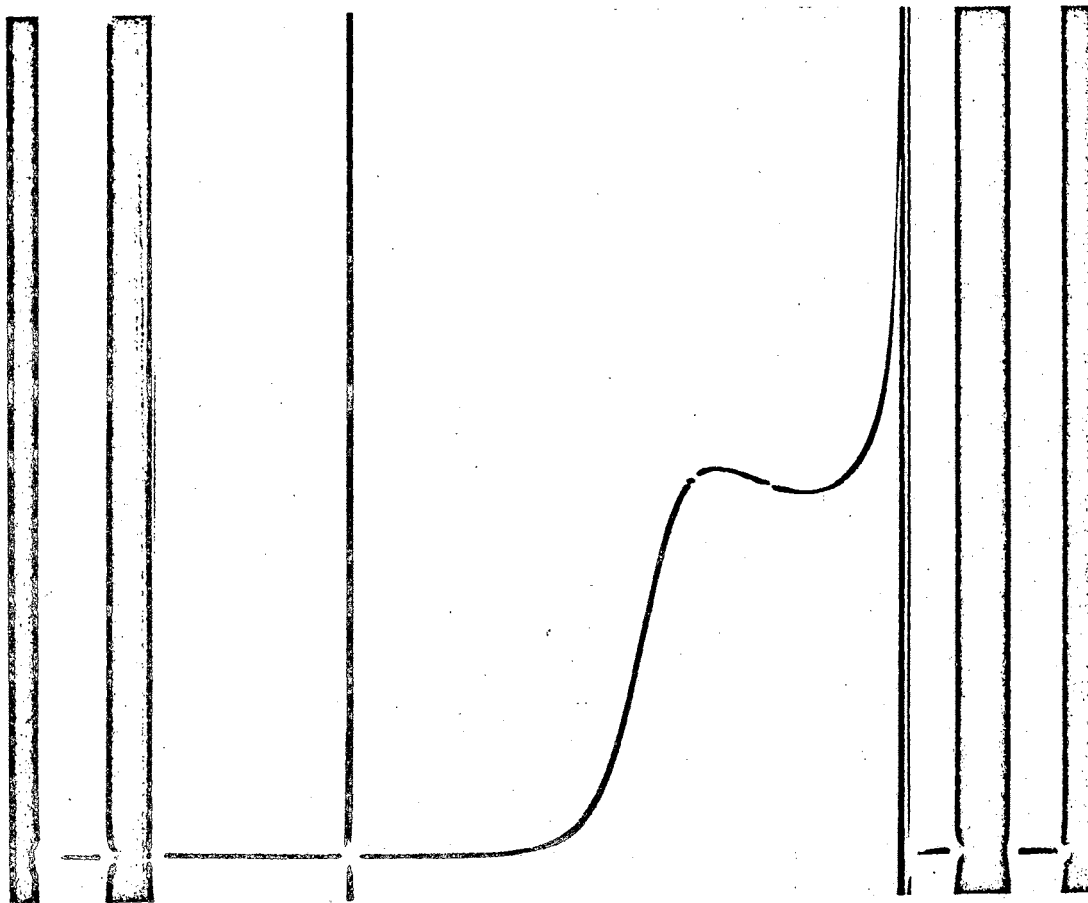


Figure 13. Schlieren Curve of the Sample Shown in Fig. 12
after Sufficient Amount of Salt Was Added.

TABLE IV. COMPARISON OF RATIOS OF EXPERIMENTALLY OBTAINED V_a WITH RATIOS OF $1/(1 + \kappa a)^2$.

Sample Number	I	II	III	IV
κ ($\times 10^6$ /cm)	2.90	4.10	5.79	9.05
Ratio of $1/(1 + \kappa a)^2$	1.00	0.68	0.44	0.23
Ratio of V_a (Expt'l)	1.00	0.69	0.51	0.29

curve shown in Fig. 13 was obtained. This curve possesses all the features of the group of curves shown in Fig. 10. The schlieren curve in Fig. 12 was believed caused by a very strong repulsive potential.

CHAPTER IV

DISCUSSIONS OF RESULTS

In Chapter II, it has been shown that if the sample is composed of fairly uniform, non-reacting macromolecules, it can be used as a probe to evaluate experimentally the interparticle interaction between macromolecules, if this interaction exists. In Chapter III, we have presented the results of the experiments on some samples of Ludox SM, whose uniformity was confirmed by a work of Alexander and Iler⁽⁵⁰⁾ using an electron microscope. In this chapter, we shall compare the interaction potential found experimentally with the ones derived from theories. The comparison will first be made against Verwey-Overbeek's two particle theory (Equations 2-11 through 2-14) and then against the simple theory suggested in Chapter II.

Comparison of Experimental and Theory

Verwey and Overbeek gave an approximate formula for two-particle interaction between charged spherical double layers⁽²³⁾. Then results were summarized in Equations (2-11) through (2-14). To check their validity, we have noted that, if the variations of β and γ in Equations (2-11) and (2-13) are ignored β and γ are slowly varying functions of interparticle distances. These parameters both have the magnitude of the order of unity. (See Reference 23 for numerical examples.) The theory predicts that the slope of a plot of V_R 's vs.

R on a semi-log paper should be $-\kappa$, where κ is the reciprocal of the Debye length. The value of κ thus obtained experimentally (cross points in Fig. 14) from the sample whose Schlieren curve was presented in Fig. 12 is $3.77 \times 10^5 \text{ cm}^{-1}$, as compared with the value of $3.9 \times 10^5 \text{ cm}^{-1}$ calculated from formula (4-1).

$$\kappa = \sqrt{\frac{2e^2V^2n}{\epsilon kT}} \quad (4-1)$$

The particle diameter obtained from the slope of the left portion of the $\log(c/c_0)$ vs. x^2 plots (see, for example, dotted line in Fig. 7) is 6.87 μ , as compared with the nominal particle diameter of 7 μ . It should be noted that errors reported in particle diameter reflect only one third of corresponding errors of molecular weight. The same good agreement was also observed between the values of $1/(1 + \kappa a)^2$ calculated via Equation (4-1) and the values of $1/(1 + \kappa a)^2$ obtained experimentally (Table IV) from repulsive potentials at the particle contact distance.

The magnitudes of the repulsive potential at contact distance ($R=2a$) obtained experimentally are, however, one order of magnitude larger than that one could expect from Equation (2-13). This discrepancy can be understood since Equation (2-13) gives only the repulsive potential between two particles, while the experimental value gives the total potential imposed upon the particle by all other particles. In fact, the ratio of these two amplitudes can be used to estimate roughly the effective nearest neighbor around a particle. In this case, the number turned out to be 11, which is also quite reasonable.

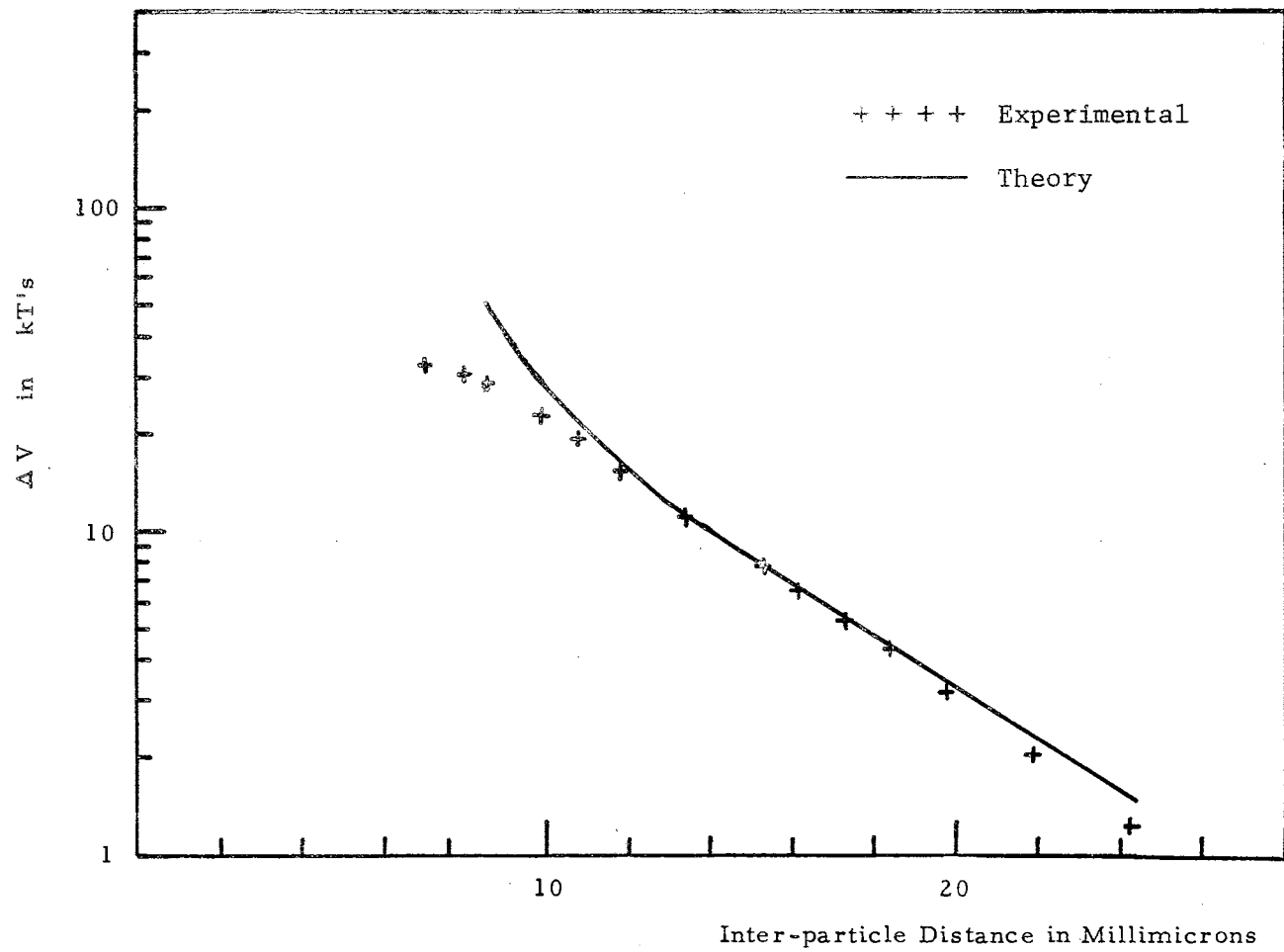


Figure 15. Comparison of Theory and Experiment.

The solid curve in Fig. 14 is obtained by calculating $V = Q(\varphi_{ab} - \varphi_{a\infty})$ where φ_{ab} is the surface electric potential of the particle when it is confined to a spherical volume of radius b . The surface term is used here because only the potential of the macromolecular particle has anything to do with the distribution of the particle. The curve was obtained by adjusting Q/κ so that the best fit possible with the experimental points at the lower concentration was obtained. However, if experimental κ value was used, the Q value required for the best fit is about 6 times smaller than that which can be expected from titration data (57, 58). Since (i) the titration data are very unreliable near the point of neutrality, and (ii) not all the surface charge sites releasable by the titration process may be available to a normal electric double layer, the author thinks there is fairly good agreement between the two surface charge densities. The solid curve begins to deviate from experimental points below 11 m μ . It bends rapidly upward as the interparticle distance decreases further. Such breakdown is understandable since the Gouy-Chapman model starts falling apart beyond this point. Future work is undoubtedly necessary to test the validity of other models.

Interaction vs. Buoyancy

There has been a great debate in the past (52) as to whether the density of the solvent or the density of the sol (solution) should be used in the calculations of the buoyancy term in the sedimentation equations such as (2-9). Equally strong arguments were presented by both sides. In the cases in which the determination of molecular

weights were the chief concern, the difference between the two points of view would not be too serious since it calls only for a correction term from each other, and this correction term is small since the concentration of the sample is low. The situation is worse in the interaction studies since it is most essential to carry out the experiments at high concentrations. The concepts of buoyancy and interparticle interaction must be clearly distinguished here. Buoyancy can only be defined if the body sees a homogeneous environment. This assumption soon breaks down when the volume of interest becomes smaller. True homogeneity does not exist in nature. The replacement of the real environment by a fictitious continuum is valid only when we can accept the average effect of the process. The average may be carried out either space-wise or time-wise. In the case of buoyancy, either the colliding particle is much smaller than the collided particle, or the collision is so frequent that we can neglect the fluctuations.

The use of apparent density (average density) to calculate the buoyancy force would break down even sooner. In the extreme case, no one would like to include the forces exerted on a glass bead near the bottom of a beaker of water by the neighboring glass beads as buoyancy. It is also hard to believe that a colloid particle which has about a dozen close neighbors would see a uniform environment during its course of Browning motion. For this reason, it is not considered good practice to include any separable interactions into the buoyancy term, nor is it necessary to introduce the concept of pseudo-buoyancy.

The ultimate proof rests on the experiments. If the observed

strangeness of the Schlieren curves were due to the buoyancy of the solution, then one would expect, after inserting the supposedly correct density, i.e., in this case, the density of the solution rather than the density of the solvent, the plot of $\log c$ vs. x^2 would return to a straight line, and this line would be independent of the very small amount of salt content in the sample, since the amount of salt will not change the density by any appreciable amount. However, we find that the observed data cannot be accounted for by manipulating the buoyancy term. The values of V_T are plotted against ρ in Fig. 1.5 for two samples which differ only in the concentration of small ions. These two samples have the same apparent density, and yet the points lie on two distinctive curves. This completely rules out the buoyancy interpretation.

Prospects of the Sedimentation-Diffusion-Interaction Equilibrium Method

In this study, it has been established that the feasibility of using ultracentrifugation techniques to map certain interactions such as the Verwey-Overbeek interaction of electric double layers. It should be pointed out here that the sedimentation-diffusion-interaction method which was used in this study for the first time, is a rather general method. In general, the shape of the Schlieren curves in the interaction zone will depend upon the nature of the interaction. It is hoped that new applications will be added to this area of study in the future. It is not at all impossible that an entirely different form of Schlieren pattern from that which has been reported here may be found in some other system.

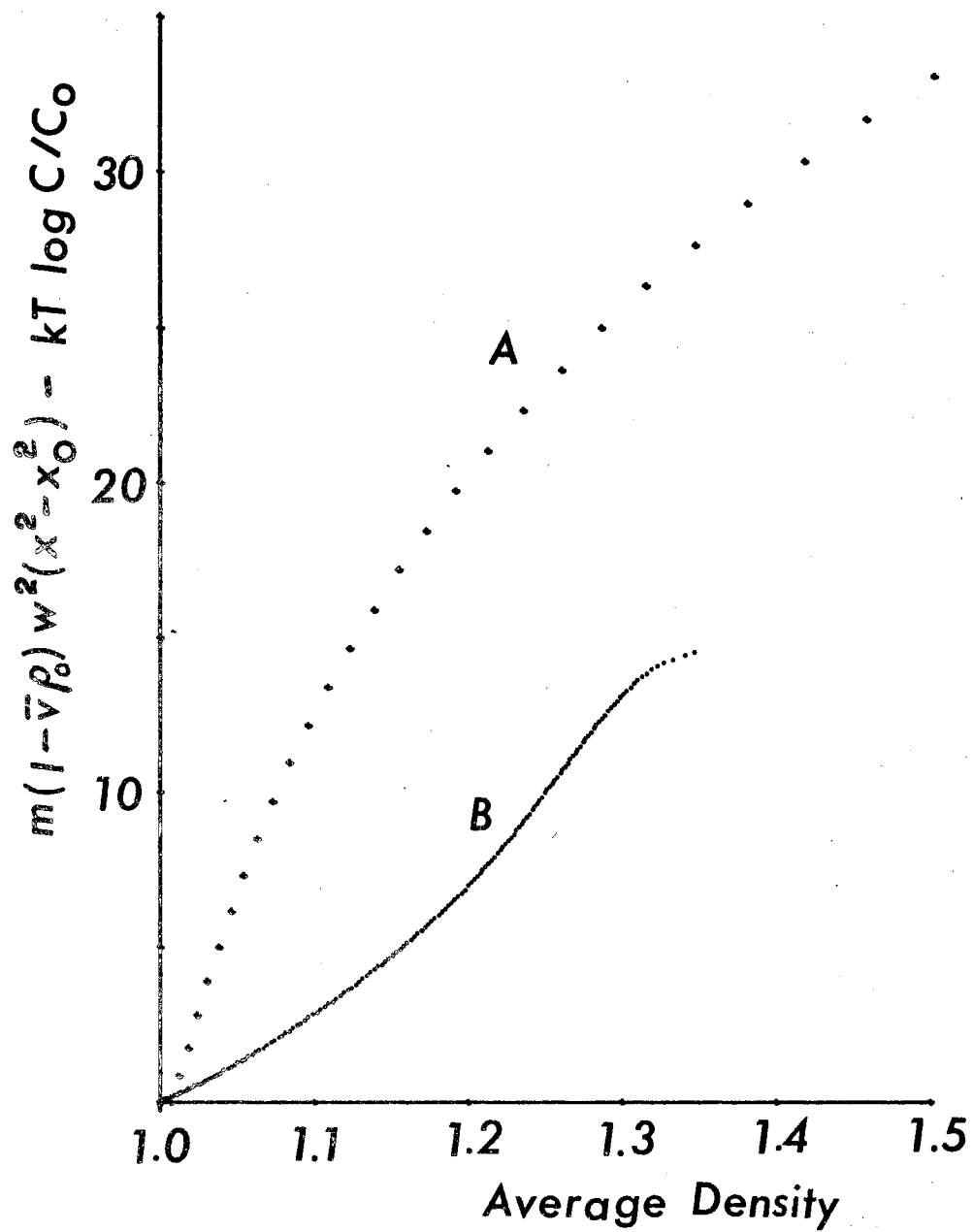


Figure 15. Comparison of Interaction Potential vs Buoyancy.

In the following, the author suggests a few problems of interest, which he feels should be investigated.

(1) Ludox SM has been used as a starting material for catalysts of controlled pore size. Kinetic studies can be carried out on coated active colloidal particles before impinging them into solids. This made the measurement of change of composition of the environment fluid at the very vicinity of the surface possible by monitoring the changes of Schlieren pattern during the course of reaction. Such an arrangement would also have the capability of studying very slow reactions.

(2) Redistribution of a third component between two immiscible liquids sometimes involves a very small amount of energy. Phase diagram data of much higher precision could be collected in these regions if ultracentrifugation were used.

(3) Temperature jump type of experiments could be carried out on the ultracentrifuge if the reaction of interest can be initialized or perturbed by a beam of very intense light, perhaps mounted at a certain degree in advance of the monitoring light beam. Information could be collected by varying the amount of perturbation and watching its effect on the Schlieren pattern.

In the history of development of NMR, realizing that nuclei can be used as probes to study the surrounding environments has brought many kinds of interesting applications. Let us hope that the same will happen at least to some extent in the field of ultracentrifugation.

A SELECTED BIBLIOGRAPHY

- (1) Svedberg, T. and H. Rinde, J. Am. Chem. Soc. 45, 2910 (1923).
- (2) Svedberg, T. and R. Fähræus, J. Am. Chem. Soc. 48, 430 (1925).
- (3) Svedberg, T. and K. O. Pederson, The Ultracentrifuge, Clarendon Press (1940), Johnson Reprint Corp. (1959).
- (4) Schachman, H. K., Ultracentrifugation in Biochemistry, Academic Press (1959).
- (5) Pickels, E. G., Chem. Rev. 30, 341 (1942).
- (6) Fujita, H., Mathematical Theory of Sedimentation Analysis, Academic Press (1962).
- (7) Williams, J. W. (Ed.), Ultracentrifugal Analysis in Theory and Experiment, Academic Press (1963).
- (8) Pedersen, Kai O., J. Phys. Chem. 62, 1282 (1958).
- (9) Reference (3), pp.23-28.
- (10) Aoki, Koichiro, J. Phys. Chem. 63, 1336 (1959).
- (11) Johnson, James S., Kurt A. Kraus, and T. Fraser Young, J. Am. Chem. Soc. 76, 1436 (1954).
- (12) Rush, Richard M., and James S. Johnson, J. Phys. Chem. 68, 2321 (1964).
- (13) Wales, Michael, J. Phys. Chem. 52, 235 (1948).
- (14) Wales, Michael, J. W. Williams, J. O. Thompson, and R. H. Ewart, J. Phys. Chem. 52, 983 (1948).
- (15) Wales, Michael, Margaret Bender, J. W. Williams, and Roswell H. Ewart, J. Chem. Phys. 14, 353 (1946).
- (16) Wales, M., J. Chem. Phys. 55, 282 (1951).
- (17) Wales, M., F. T. Adler, and K. E. van Holde, J. Phys. Chem. 55, 145 (1951).

- (18) Wales, M., *J. Applied Phys.* 22, 735 (1951).
- (19) Erlander, Stig R., *Iowa State J. Sci.* 38, 323 (1964).
- (20) Erlander, Stig R., and F. R. Senti, *Makromol. Chem.* 73, 14 (1964).
- (21) Erlander, Stig R., and F. R. Senti, *Makromol. Chem.* 73, 31 (1964).
- (22) Goldberg, Richard J., *J. Phys. Chem.* 57, 194 (1953).
- (23) Verwey, E. J. W., and J. Th. G. Overbeek, Theory of the Stability of Lyophobic Colloids (Elsevier Pub. Co., 1948).
- (24) Deryagin, B. V., and L. D. Landau, *Acta Physicochim. USSR*, 14, 663 (1941); *Zh. Eksperim. i Teor. Fiz.* 15, 663 (1945).
- (25) Deryagin, *Trans. Faraday Soc.* 36, 203 (1940); 36, 730 (1940).
- (26) Grahame, D. C., *J. Am. Chem. Soc.* 76, 4819 (1954).
- (27) Li, Hsiao-Yuan, unpublished, M. S. Thesis, Oklahoma State University (1966).
- (28) Matsukura, Yasuo, *Japan. J. Appl. Phys.* 3, 409 (1964).
- (29) Ray, B. Roger, Donald M. Beeson, and Harold F. Crandall, *J. Phys. Chem.* 80, 1029 (1958).
- (30) Gouy, G., *J. physique* 9, 457 (1910); *Ann. d. phys.* 7, 129 (1917).
- (31) Chapman, D. L., *Philos. Mag.* 25, 475 (1913).
- (32) Stern, O., *Z. Elektrochem.* 30, 508 (1924).
- (33) Delahay, Paul, Double Layer and Electrode Kinetics, (Interscience Publ., 1965).
- (34) Deryagin, B. V. (Ed.), Research in Surface Forces, Vol. II, (Translated from Russian, Consultant Bureau, 1966).
- (35) Li, Hsiao-Yuan, and Victor L. Pollak, Abstracts of Papers, COLL-011, Division of Colloid and Surface Chemistry, 156th National Meeting, American Chemical Society, Atlantic City, September, 1968.
- (36) Loeb, A. L., J. Th. G. Overbeek, and P. H. Wiersema, The Electrical Double Layer Around a Spherical Colloid Particle, (The M. I. T. Press, 1961).

- (37) P. 56 and p. 58 of Reference 23.
- (38) Levine, S., Trans. Faraday Soc. 42B, 102 (1946); 44, 833 (1948).
- (39) Levine, S., Phil. Mag. 41, 53 (1950).
- (40) Levine, S., Proc. Cambridge Phil. Soc. 47, 217 (1951); 47, 230 (1951).
- (41) Levine, S., J. Colloid Sci. 6, 1 (1951).
- (42) Levine, S., Proc. Phys. Soc. 64A, 781 (1951).
- (43) Ikeda, Yuichi, J. Phys. Soc. Japan 8, 49 (1953).
- (44) Stratton, Julius Adams, Electromagnetic Theory, p. 107, (McGraw-Hill, 1941).
- (45) See, for example, the Beckman Model E Manual.
- (46) Fixman, Marshall, J. Phys. Chem. 62, 374 (1958).
- (47) Bechtold, M. F. and O. E. Snyder, U. S. Pat. 2,574,902 (1949).
- (48) Rule, J. M., U. S. Pat. 2,577,485 (1951).
- (49) Maron, Samuel H. and Richard L. H. Lou, J. Polymer Sci. 14, 29 (1954).
- (50) Alexander, G. B., and R. K. Iler, J. Phys. Chem. 57, 932 (1953).
- (51) Bell, G. M. and S. Levine, J. Chem. Phys. 49, 4584 (1968).
- (52) Hermans, J. J., Makromol. Chem. 74, 92 (1964).
- (53) Nichol, L. W., A. G. Ogston, and B. N. Preston, Biochem. J. 102, 407 (1967).
- (54) Gofman, J. W., E. T. Lindgren, and H. Elliott, J. Biol. Chem. 179, 973 (1949).
- (55) Ikeda, Shoichi and Kinji Kakiuchi, J. Colloid and Interface Sci. 23, 134 (1967).
- (56) Bolt, G. H., J. Phys. Chem. 61, 1166 (1957).
- (57) Hester, W. M., Jr., R. K. Iler, and G. W. Sears, Jr., J. Phys. Chem. 64, 147 (1960).

VITA 3

Hsiao-Yuan Li

Candidate for the Degree of
Doctor of Philosophy

Thesis: STUDY OF REPULSIVE INTERACTION BETWEEN COLLOIDAL PARTICLES BY
MEANS OF SEDIMENTATION-DIFFUSION-INTERACTION EQUILIBRIUM UNDER
ULTRACENTRIFUGATION

Major Field: Physics

Biographical:

Personal Data: Born in Hongchow, Chekiang, China, July 9, 1935,
the son of Mr. and Mrs. Ker-Yuan Li. Migrated to Taiwan in
the Spring of 1949.

Education: Attended grade school in Chengtu, Szechwan; and junior
high school in Hongchow, Chekiang; graduated from Provincial
Kangshan Senior High School, Kangshan, Taiwan in February,
1953; received a Bachelor of Science in Engineering degree
from National Taiwan University, Taipei, Taiwan, in June,
1957, with a major of Chemical Engineering; received a Master
of Science degree in Oklahoma State University in May, 1966,
with a major of Physics; completed requirements for the Doc-
tor of Philosophy degree at Oklahoma State University in
August, 1969.

Organizations: Member of Sigma Pi Sigma, member of the American
Physical Society, associate member of the American Chemical
Society, and associate member of the Society of Sigma Xi.